frontiers in Physics

REVIEW
published: 28 January 2020
doi: 10.3389/fphy.2020.00001

NN Scattering and Nuclear Uncertainties

Enrique Ruiz Arriola[1]*, *Jose Enrique Amaro*[1]* and *Rodrigo Navarro Pérez*[2]

[1] Departamento de Física Atómica, Molecular y Nuclear and Instituto Carlos I de Física Teórica y Computacional, Universidad de Granada, Granada, Spain, [2] Department of Physics, San Diego State University, San Diego, CA, United States

Ab initio calculations in Nuclear physics for atomic nuclei require a specific knowledge of the interactions among their constituents, protons and neutrons. In particular, NN interactions can be constrained down to scale resolutions of $\Delta r \sim 0.6$ fm from the study of phase shifts below the pion production threshold. However, this allows for ambiguities and uncertainties which have an impact on finite nuclei, nuclear- and neutron-matter properties. On the other hand the nuclear many body problem is intrinsically difficult and the computational cost increases with numerical precision and number of nucleons. However, it is unclear what the physical precision should be for these calculations. In this contribution we review much of the work done in Granada to encompass both the uncertainties stemming from the NN scattering database in light nuclei such as triton and alpha particle and the numerical precision required by the solution method.

Keywords: nucleon-nucleon interaction, scattering data, uncertainty quantification, nuclear binding, effective interactions, statistical analysis

OPEN ACCESS

Edited by:
Ruprecht Machleidt,
University of Idaho, United States

Reviewed by:
Victor Mokeev,
Thomas Jefferson National Accelerator Facility, United States
Roelof Bijker,
National Autonomous University of Mexico, Mexico

***Correspondence:**
Enrique Ruiz Arriola
earriola@ugr.es
Jose Enrique Amaro
amaro@ugr.es

Specialty section:
This article was submitted to Nuclear Physics, a section of the journal Frontiers in Physics

Received: *21 November 2019*
Accepted: *06 January 2020*
Published: *28 January 2020*

Citation:
Ruiz Arriola E, Amaro JE and Navarro Pérez R (2020) NN Scattering and Nuclear Uncertainties. Front. Phys. 8:1. doi: 10.3389/fphy.2020.00001

1. INTRODUCTION

One of the main goals in Theoretical Nuclear Physics for many years has been to achieve a sufficiently accurate *ab initio* solution of the Nuclear Many Body Problem from a reductionist perspective. Within the present context this means starting with the forces among the hadronic constituents, protons and neutrons, and solving the corresponding quantum mechanical problem. While this has been widely and openly recognized as an extremely difficult problem, it already represents a simplification as compared to the fundamental problem where the constituents are quarks and gluons building the nucleons and the interactions are deduced from the gauge principle in QCD. The nuclear problem schematically comprises two main steps (i) the determination of the basic interactions from spectroscopy and reactions at the few body level and (ii) a precise method of solution of the inferred interactions for the many body problem. The predictive power of the theory corresponds therefore to the relation between the input (nuclear two-, three-, four-body, and so on, forces) and the output nuclear binding energies, form factors and nuclear reactions, and the corresponding uncertainties.

The seminal paper of Yukawa [1] established the first theoretical evidence that the nuclear force has a finite range by the particle exchange mechanism. The first determination of the tensor force and its consequences for the deuteron were analyzed by Bethe [2, 3]. The first χ^2 statistical analyzes of NN scattering data below pion production threshold started in the mid fifties [4] (an account up to 1966 can be traced from Arndt and Macgregor [5]). A modified χ^2 method was introduced [6] in order to include data without absolute normalization. The steady increase along the years in the number of scattering data with better precision generated incompatibilities and hence different criteria had to be introduced [7–9] to discard inconsistent data. For a comprehensive review up to 1977 see [10–13]. For a historical presentation before 1989 we recommend Machleidt [14].

Error analysis of NN phase-shifts for several partial waves became first possible when the Nijmegen group [15] carried out a partial wave analysis (PWA) fitting about 4,000 experimental np and pp data, after rejecting about 1,000 inconsistent data with a 3σ criterion. The analysis resulted in a value $\chi^2/\text{dof} \sim 1$. In the fit the potential was an energy dependent square well of radius 1.4 fm, plus one-pion-exchange (OPE) and charge-dependent (CD) contributions starting at 1.4 fm, and a one-boson-exchange (OBE) piece operating below 2–2.5 fm. Unfortunately, the required energy dependence becomes messy for nuclear structure calculations. In the next decade a variety of NN (energy independent) potentials appeared in the literature fitting a large body of scattering data with $\chi^2/\text{dof} \sim 1$ [15–19], but surprisingly error estimates on potential parameters were not made. While all these modern potentials share the *local* OPE and CD tail and include electromagnetic effects, the unknown short range components of these potentials display a variety of forms and shapes: local potentials [16], non-local ones with angular momentum dependence [17], energy dependence [15], or momentum dependence [16, 18, 19]. While in principle $p-$, $L-$, and $E-$non-localities are equivalent on-shell (see e.g., Amghar and Desplanques [20] for a proof in a $1/M_N$ expansion) they reflect truly different physical effects and generally one should consider them as independent quantities. Any specific choice results in a bias and hence becomes a source of systematic errors.

Error propagation from nucleon-nucleon data to three- and four-nucleon binding energies was pioneered in Adam et al. [21]. A rudimentary method based on coarse grained NN interactions was proposed [22, 23] providing a first guess for error on bindings in nuclei and neutron and nuclear matter. The Granada analysis of the triton using hyper-spherical harmonics method was performed in Navarro Perez et al. [24]. The triton and the alpha particle were analyzed by solving the Faddeev equations for ^{3}H and the Yakubovsky equations for ^{4}He in [25], and in *ab initio* no-core full configuration calculations [26]. Theoretical uncertainties in the elastic nucleon-deuteron scattering observables were calculated in Skibinski et al. [27].

While the history of the NN force and its applications to nuclear physics is rather long, uncertainty quantification has not been addressed seriously until recently (see e.g., [28] for a review prefacing a full volume of the ISNET community). There are several reasons why we think that stressing this aspect of the theory may be particularly useful and fruitful. One obvious one is to provide sensible error estimates in the theoretical calculations. The traditional way was to try out several schemes and compare the different results. Another, less obvious reason, is to address the many body nuclear problem within the realistic physical accuracy, rather than the computational accuracy as it has been the customary approach up to now. This applies in particular to the a priori accuracy of the solution of the nuclear many body problem, which may eventually be relaxed as to facilitate calculations not addressed before. However, this may occur at a high price; it is not unthinkable that any realistic attempt to quantify the theoretical uncertainties may end up with a lack of predictive power on the side of the theory.

We distinguish as usual in error analyses two sources of uncertainties: statistical errors stemming from the data uncertainties for a *fixed* form of the potential, and systematic errors arising from the *different* most-likely forms of the potentials. Assuming they are independent, the total uncertainty corresponds to adding both uncertainties in quadrature. In what follows it is advantageous to take the viewpoint of considering any of the different potentials as an independent but possibly *biased* way to determine the scattering amplitudes and/or phase-shifts. Because the biases introduced in all single potential are independent on each other, a randomization of systematic errors makes sense.

A prerequisite for such an analysis is to discern as much as possible between statistical and systematic uncertainties. The former correspond to the proper propagation of the experimental input while the latter is concerned with the model or scheme dependence of the calculation procedure. Systematic errors may include the genuine bias to describe the physics and truncation errors which are related to the approximate way the calculation is carried out. At the present stage, the model bias is the largest source of uncertainty.

After many years of tremendous efforts and steady progress, state of the art calculations suggest that considerable success can be expected if one includes the current knowledge of the two-, three-body forces and a variety of many body techniques are applied. Going beyond four-body forces has never been tried out, partly because of technical difficulties but also because of the appearance of $\alpha-$clustering, based on the large stability and compactness of the ^{4}He nucleus, suggests that five body forces are marginal[1].

As already said, a credible quantification of the accuracy of the theory requires a judicious determination of all sources of error in the final results, including both the experimental information needed to pin down the interactions as well as the convergence of the numerical procedure used to solve the many body problem. Given the formidable computational effort needed to implement accurately many body calculations—even for light nuclei—an *a priori* determination of the errors induced from input data would very helpful. This would set an useful accuracy goal and a limit beyond which all refinements in the numerics would not improve the *theoretical* accuracy of the output. The purpose of the present work is to review estimates on such limiting accuracy based on the imperfect knowledge of the basic two body interactions.

Unfortunately, the situation we face in strong interactions in general and in nuclear physics in particular is to compare and validate inaccurate theories on the basis of accurate data. No theoretical predictions outperforming experimental measurements in accuracy are easily found. To make our point and concern more clear let us take for instance the case of nuclear binding energies from a *semi-empirical* point of view, where a direct reference to nuclear forces is mostly avoided. Bindings are experimentally known to high accuracy, $\Delta B = 0.01 - 10$ KeV, whereas liquid-drop model inspired mass fit formulas yield a lower theoretical accuracy $\Delta B = 0.6$ MeV (see e.g., Toivanen et al. [29] and references therein). This suggests that already

[1] Actually there are no purely contact interactions beyond four body ones for fields with $(n, p, \uparrow, \downarrow)$ degrees of freedom.

within such a simple picture the phenomenological theory is generally *not expected* to be more accurate in its predictions than experiment. Actually, according to the standard $\chi^2/\text{dof} \sim 1$ criterion the previous results show that the theory is literally *incompatible* with data, and thus not even an error analysis based on uncertainty propagation may be undertaken. The situation is presumably less optimistic for the *ab initio* approach based entirely on the knowledge of (multiparticle) nuclear forces and a skillful solution of the nuclear many body problem. This provides a motivation to quantify the accuracy needed to solve the many body problem.

2. STATEMENT OF THE PROBLEM

Let us be more specific on the meaning of uncertainty quantification in nuclear physics. From a Hamiltonian describing A-nucleons, H_A, with kinetic energy $T = \sum_{i=1}^{A} p_i^2/2M$ and multi-nucleon forces V_{nN},

$$H_A = T + V_{2N} + V_{3N} + V_{4N} + \ldots, \tag{1}$$

where

$$V_{2N} = \sum_{i<j} V_{ij}\,, \quad V_{3N} = \sum_{i<j<k} V_{ijk}\,, \quad V_{4N} = \sum_{i<j<k<l} V_{ijkl} \quad \ldots \tag{2}$$

one proceeds to solve the Schrödinger equation

$$H_A \Psi_n = E_{n,A} \Psi_n. \tag{3}$$

In the absence of useful and accurate QCD-*ab initio* determinations, phenomenological V_{2N} interactions are *adjusted* to NN scattering data and the deuteron, ^{2}H ($A = 2$), binding energy, while V_{3N} enter into the ^{3}H and ^{3}He ($A = 3$), bindings, V_{4N} in ^{4}He (A = 4), and so on. Thus, the theoretical predictive power flow is expected to be from light to heavy nuclei. For instance, in the case of the binding energy the problem of error propagation based on NN force variations corresponds to

$$V_{NN} = \bar{V}_{NN} \pm \Delta V_{NN} \to E_n(A) = \bar{E}_n(A) \pm \Delta E_n(A) \tag{4}$$

The meaning of the variation ΔV_{NN} is a bit subtle, since there are variations which are (scattering) equivalent and hence do not change the scattering observables.

We are interested firstly in the NN scattering problem [30]. Quite generally we will consider non-relativistic scattering of two particles with masses m_1 and m_2 where $H = H_0 + V$ and $H_0 = p^2/2\mu$ is the kinetic energy and $\mu = m_1 m_2/(m_1 + m_2)$ the reduced mass (we drop "*NN*" for simplicity). The S-matrix is defined as a boundary condition problem for $E \geq 0$

$$S(E + i\epsilon) = 1 - 2\pi i \delta(E - H_0) T(E + i\epsilon) \tag{5}$$

where we have introduced the T-matrix which satisfies the scattering equation in operator form,

$$\begin{aligned} T(E) &= V + V G_0(E) T(E) \\ &= V + V G_0(E) V + \cdots = V(1 - G_0(E) V)^{-1} \end{aligned} \tag{6}$$

where in the second equality we write the exact summation of the perturbative series. Other (complex) energy values are defined by analytical continuation. The T-matrix satisfies the reflection property $T(E + i\epsilon)^\dagger = T(E - i\epsilon)$ if $V = V^\dagger$ in Equation (6) and hence the unitarity condition, $S(E + i\epsilon) S(E + i\epsilon)^\dagger = 1$, follows also from $V = V^\dagger$ in Equation (6). The phase-shift is defined in terms of the eigenvalues of the S-matrix, so that $S\varphi_\alpha = e^{2i\delta_\alpha}\varphi_\alpha$ and for rotational invariant interactions (we neglect spin to ease the notation) the scattering amplitude $M(\mathbf{p}', \mathbf{p})$ is given by

$$\begin{aligned} M(\mathbf{p}', \mathbf{p}) &= \sum_{lm} 4\pi\, Y_{lm}(\mathbf{p}) Y_{lm}(\mathbf{p}') \frac{e^{i\delta_l(p)} \sin\delta_l(p)}{p} \\ &= -\frac{2\mu}{4\pi} \langle \vec{p}\,' | T(E + i\epsilon) | \vec{p} \rangle \Big|_{E_p = E_{p'} = E} \end{aligned} \tag{7}$$

with $Y_{lm}(\mathbf{p})$ the spherical harmonics and in our convention $d\sigma/d\Omega = |M(\mathbf{p}', \mathbf{p})|^2$ the differential cross section. Any *NN* unitary transformation, U, transforms the Hamiltonian and hence the potential as $V \to \tilde{V} = UHU^\dagger - H_0$. For an infinitesimal transformation $U = 1 + i\eta + \ldots$, where η is a small self-adjoint two-body operator, the scattering equivalent variation corresponds to the change $\Delta V = i[\eta, H]$. To see the effect on scattering, start with the LS equation in the form $T^{-1} = V^{-1} - G_0$ which upon a variation of the potential produces a variation of the T-matrix $\Delta T = TV^{-1}\Delta V V^{-1} T$ and after some manipulation one gets

$$-i\Delta T = (1 + TG_0)\eta G_0^{-1} - G_0^{-1}\eta(1 + G_0 T) \tag{8}$$

so that sandwiching this expression between plane waves gives

$$\begin{aligned} \Delta\langle \vec{k}\,' | T(E + i\epsilon) | \vec{k} \rangle = &-i(E - E_{k'} + i\epsilon)\langle k' | \eta(1 + G_0 T) | k \rangle \\ &+ i(E - E_k + i\epsilon)\langle k' | (1 + TG_0)\eta | k \rangle \end{aligned} \tag{9}$$

which vanishes in the on-shell limit $E_k = E_{k'} = E$ and $\epsilon \to 0$. Thus,

$$\Delta V = i[\eta, H] \implies \Delta\langle \vec{k}\,' | T(E + i\epsilon) | \vec{k} \rangle \Big|_{E_k = E_{k'} = E} = 0 \tag{10}$$

or equivalently for finite unitary transformations, using Equation (7), $\delta_{l,H}(p) = \delta_{l,UHU^\dagger}(p)$.

Given this general ambiguity the long lasting problem has been to decide which is the proper representation of the NN interaction based on NN scattering data. This is in essence the so-called inverse scattering problem which has been studied extensively in the past (see e.g., Chadan and Sabatier [31] and Newton [32] for reviews)] and requires additional strong assumptions to fix the particular form of the potential. For instance, assuming a *local* potential and *complete* knowledge of the phase-shifts in each partial wave it is possible to determine the solution uniquely provided the binding energies and long distance behavior of the corresponding bound states wave functions allocated by the potential are known. Clearly, these inverse scattering ambiguities have an impact on the solution of the many body problem, as was documented long time ago in nuclear matter [33] and in the triton and alpha particles [34],

just to mention two prominent examples (see Srivastava and Sprung [35] for a review).

Much of the arbitrariness is reduced by invoking an underlying theoretical description in terms of hadronic degrees of freedom, which allows to compute $V_{NN}(\vec{x})$ in terms of one-, two-,..., pion exchanges. which in turn may be related to the πN scattering process, involving coupling constants for vertex interactions. At present such a picture seems to hold down to NN separations of about the elementary radius, $r_c = 1.8$ fm, below which composite and finite size effects start playing a role That means that, essentially, variations of the NN potential of are restricted at least to $\Delta V_{NN}(\vec{x}) = 0$ for $r \geq r_c \approx 1.8$ fm.

3. THE NN POTENTIAL

3.1. The Concept of a Potential

In order to properly formulate the uncertainties of the potentials it would be adequate to review first the meaning of a potential in nuclear physics. This is of utmost importance but also intriguing. On the one hand the potential is not an observable but on the other hand to our knowledge it is not practical to carry out *ab initio* calculations in Nuclear Physics at the hadronic level without potentials. Ultimately, one hopes to be able to provide a direct link between the uncertainties in the input data and propagate them to the output of the many body problem. As said, this is only possible by using non-observable nuclear potentials as intermediate steps.

From a classical (and macroscopic) point of view, potential and force can be measured directly by just determining the separation static energy between two infinitely heavy sources. Such a definition admits a direct extension to the quantum mechanical microscopic case and specifically to the NN interaction assuming interpolating composite local nucleon fields made out of three quarks. In essence, this is the approach followed in recent years in lattice QCD where many of the traditionally assumed features of the NN interaction seem to be confirmed [36–38]. A major drawback of this approach is that such a calculation determines the static NN energy which would become a physical observable if nucleons were infinitely heavy. The quantum mechanical problem needs adding kinetic energy contributions. Moreover, the fact that low energy NN scattering provides unnaturally large cross sections corresponds to an extreme fine tuning which is beyond the present lattice capabilities.

3.2. The Tensorial Structure

Assuming isospin invariance for the moment, the most general form of the NN interaction can be written as Okubo et al. [39]

$$\begin{aligned} V(\mathbf{p}',\mathbf{p}) = \; & V_C \; + \vec{\tau}_1\cdot\vec{\tau}_2\, W_C + \left[\, V_S \; + \vec{\tau}_1\cdot\vec{\tau}_2\, W_S \;\right] \vec{\sigma}_1\cdot\vec{\sigma}_2 \\ & - i\vec{S}\cdot(\mathbf{q}\times\mathbf{P})\left[\, V_{LS} + \vec{\tau}_1\cdot\vec{\tau}_2\, W_{LS}\right] \\ & + \left[\, V_T \; + \vec{\tau}_1\cdot\vec{\tau}_2\, W_T \;\right] \vec{\sigma}_1\cdot\mathbf{q}\;\vec{\sigma}_2\cdot\mathbf{q} \\ & + \left[\, V_Q + \vec{\tau}_1\cdot\vec{\tau}_2\, W_Q \,\right] \vec{\sigma}_1\cdot(\mathbf{q}\times\mathbf{P})\;\vec{\sigma}_2\cdot(\mathbf{q}\times\mathbf{P}) \\ & + \left[\, V_P + \vec{\tau}_1\cdot\vec{\tau}_2\, W_P \,\right] \vec{\sigma}_1\cdot\mathbf{P}\;\vec{\sigma}_2\cdot\mathbf{P}\,, \end{aligned} \tag{11}$$

where $\mathbf{p}'$ and $\mathbf{p}$ denote the final and initial nucleon momenta in the CMS, respectively. Moreover, $\mathbf{q} = \mathbf{p}' - \mathbf{p}$ is the momentum transfer, $\mathbf{P} = (\mathbf{p}' + \mathbf{p})/2$ the average momentum, and $\vec{S} = (\vec{\sigma}_1 + \vec{\sigma}_2)/2$ the total spin, with $\vec{\sigma}_{1,2}$ and $\vec{\tau}_{1,2}$ the spin and isospin operators, of nucleon 1 and 2, respectively.

The scalar functions appearing in the potential, Equation (11), depend on *both* initial and final momentum $\mathbf{p}$ and $\mathbf{p}'$ respectively. Because of rotational invariance we may thus form three independent invariants, such as p, p' and also $\mathbf{q}\cdot\mathbf{P}$ (which vanishes on-shell). Transforming to coordinate space in the variable $\mathbf{r}$, conjugate to q, we have

$$V(\mathbf{r},\mathbf{P}) = \int \frac{d^3q}{(2\pi)^3} e^{i\mathbf{q}\cdot\mathbf{r}} \langle \mathbf{P} + \tfrac{1}{2}\mathbf{q}|V|\mathbf{P} - \tfrac{1}{2}\mathbf{q}\rangle, \tag{12}$$

where we take $\langle \mathbf{P} + \frac{1}{2}\mathbf{q}|V|\mathbf{P} - \frac{1}{2}\mathbf{q}\rangle \equiv V(\mathbf{p}',\mathbf{p})$. The case where these functions depend *only* on the momentum transfer $\mathbf{q} = \mathbf{p}' - \mathbf{p}$ corresponds in coordinate space to a *local* potential, $V(\mathbf{r},\mathbf{P}) = V(\mathbf{r})$. Local potentials are appealing because they provide physical insight besides being directly manageable by means of a Schrödinger equation in configuration space. Moreover, attaching a field theoretical interpretation to the interaction, locality must be satisfied by heavy and point-like elementary nucleons which act as static sources, so that in this case the potential becomes the static energy between nucleons which is an unique observable defined by

$$E_{NN}(r) = V_{NN}(r) + 2M_N + \mathcal{O}(M_N^{-1}), \tag{13}$$

where we assume $M_N \gg m_\pi, E$. Non-localities are expected to be weak because $P/M_N \ll 1$, and should have a larger influence at short distances (see e.g., Piarulli et al. [40] for an explicit implementation). The finite mass effects generate some ambiguity in the definition of the potential and, as we will see, are the largest source of uncertainties in nuclear physics. In any case, there is some freedom that can be used advantageously to *choose*—by means of suitable unitary transformations [41]—a convenient form of the potential to simplify the solution of the two-body problem, and to simplify a particular scheme of the many body problem. We remind, however, that this choice may be a source of bias and hence of systematic uncertainty.

3.3. Operator Basis

In our analysis we will be using potentials which become local in the partial wave basis. While the use of local potentials is very appealing since the whole analysis simplifies tremendously, the truth is that their use at all distances is questionable for extended particles. However, the range of non-locality is determined by the interaction and our analysis (see below) supports that on a scale $\Delta r \sim 0.6$ fm non-locality is not essential.

The potential is written as a sum of functions multiplied by each operator

$$V(r) = \sum_{n=1,23} V_n(r) O^n \tag{14}$$

The first 14 operators are charge independent and correspond to the ones used in the Argonne v_{14} potential

$$\begin{aligned} O^{n=1,14} =& 1, \tau_1\cdot\tau_2,\ \sigma_1\cdot\sigma_2, (\sigma_1\cdot\sigma_2)(\tau_1\cdot\tau_2),\ S_{12}, S_{12}(\tau_1\cdot\tau_2), \\ & \mathbf{L}\cdot\mathbf{S}, \mathbf{L}\cdot\mathbf{S}(\tau_1\cdot\tau_2), L^2, L^2(\tau_1\cdot\tau_2),\ L^2(\sigma_1\cdot\sigma_2), \\ & L^2(\sigma_1\cdot\sigma_2)(\tau_1\cdot\tau_2),\ (\mathbf{L}\cdot\mathbf{S})^2, (\mathbf{L}\cdot\mathbf{S})^2(\tau_1\cdot\tau_2). \end{aligned} \tag{15}$$

These 14 components are denoted by c, τ, σ, $\sigma\tau$, t, $t\tau$, ls, $ls\tau$, $l2$, $l2\tau$, $l2\sigma$, $l2\sigma\tau$, $ls2$, and $ls2\tau$. The remaining CD operators are

$$\begin{aligned} O^{n=15,21} =& T_{12}, (\sigma_1\cdot\sigma_2)T_{12}, S_{12}T_{12}, (\tau_{z1}+\tau_{z2}), \\ & (\sigma_1\cdot\sigma_2)(\tau_{z1}+\tau_{z2}), L^2T_{12}, L^2(\sigma_1\cdot\sigma_2)T_{12}, \\ & \mathbf{L}\cdot\mathbf{S}T_{12}, (\mathbf{L}\cdot\mathbf{S})^2T_{12} \end{aligned} \tag{16}$$

and are labeled as T, σT,tT, τz,$\sigma\tau z$, $l2T$, $l2\sigma T$, lsT, and $ls2T$. The first five were introduced by Wiringa et al. [17]; the following two were included in Navarro Pérez et al. [42] to restrict CD to the $^1S_0$ partial wave by following certain linear dependence relations between V_T, $V_{\sigma T}$, V_{l2T}, and $V_{l2\sigma T}$. The last two terms are required for the CD on the $^3P_0$, $^3P_1$, and $^3P_2$ partial waves. To incorporate CD on P waves two more operators need to be added to the basis we used previously getting a total of 23 operators O^n.

As in our previous analysis we set $V_{tT} = V_{\tau z} = V_{\sigma\tau z} = 0$ to exclude CD on the tensor terms and charge asymmetries. To restrict CD to the S and P waves parameters the remaining potential functions must follow

$$48V_{l2T} = -5V_T + 3V_{\sigma T} + 12V_{lsT} - 48V_{ls2T} \tag{17}$$

$$48V_{\sigma l2T} = V_T - 7V_{\sigma T} + 4V_{lsT} - 16V_{ls2T} \tag{18}$$

The algebraic relation between the operator basis in momentum space and in configuration space is explicitly given in Navarro Perez and Ruiz Arriola [43] and several examples are displayed.

3.4. The Long Range Contributions

As mentioned above, the potential becomes an observable within a QFT setup for infinitely heavy hadronic sources. For the finite mass case one may use instead a perturbative matching procedure between a QFT with hadronic (and electro-magnetic fields) fields and the quantum mechanical problem, which should work at sufficiently long distances. The hadronic QFT calculable contribution is separated into two pieces, the strong (pion exchange) piece and the purely EM piece,

$$V_{\rm QFT} = V_\pi(r) + V_{\rm EM}(r)\,. \tag{19}$$

The CD-OPE potential in the long range part of the interaction is the same as the one used by the Nijmegen group on their 1993 PWA [15] and reads

$$V_{m,\rm OPE}(r) = f^2\left(\frac{m}{m_{\pi^\pm}}\right)^2 \frac{1}{3} m\left[Y_m(r)\sigma_1\cdot\sigma_2 + T_m(r)S_{1,2}\right] \tag{20}$$

being f the pion coupling constant, σ_1 and σ_2 the single nucleon Pauli matrices, $S_{1,2}$ the tensor operator, $Y_m(r)$ and $T_m(r)$ the usual Yukawa and tensor functions,

$$Y_m(r) = \frac{e^{-mr}}{mr},$$

$$T_m(r) = \left(1 + \frac{3}{mr} + \frac{3}{(mr)^2}\right)\frac{e^{-mr}}{mr}. \tag{21}$$

CD is introduced by the difference between the charged $m_{\pi^\pm}$ and neutral m_{π^0} pion mass by setting

$$\begin{aligned} V_{\rm OPE,}pp(r) &= V_{m_{\pi^0},\rm OPE}(r), \\ V_{\rm OPE,}np(r) &= -V_{m_{\pi^0},\rm OPE}(r) + (-)^{(T+1)}2V_{m_{\pi^\pm},\rm OPE}(r). \end{aligned} \tag{22}$$

The neutron-proton electromagnetic potential includes only a magnetic moment interaction

$$V_{\rm EM,np}(r) = V_{\rm MM,np}(r) = -\frac{\alpha\mu_n}{2M_n r^3}\left(\frac{\mu_p S_{1,2}}{2M_p} + \frac{\mathbf{L}\cdot\mathbf{S}}{\mu_{np}}\right), \tag{23}$$

where μ_n and μ_p are the neutron and proton magnetic moments, M_n the neutron mass, M_p the proton one and $\mathbf{L}\cdot\mathbf{S}$ is the spin orbit operator. The EM terms in the proton-proton channel include one and two photon exchange, vacuum polarization and magnetic moment,

$$V_{\rm EM,pp}(r) = V_{\rm C1}(r) + V_{\rm C2}(r) + V_{\rm VP}(r) + V_{\rm MM,pp}(r) \tag{24}$$

where

$$V_{\rm C1}(r) = \frac{\alpha'}{r}, \tag{25}$$

$$V_{\rm C2}(r) = -\frac{\alpha\alpha'}{M_p r^2}, \tag{26}$$

$$V_{\rm VP}(r) = \frac{2\alpha\alpha'}{3\pi r}\int_1^\infty e^{-2m_e rx}\left(1+\frac{1}{2x^2}\right)\frac{\sqrt{x^2-1}}{x^2}dx, \tag{27}$$

$$V_{\rm MM,pp}(r) = -\frac{\alpha}{4M_p^2 r^3}\left[\mu_p^2 S_{1,2} + 2(4\mu_p - 1)\mathbf{L}\cdot\mathbf{S}\right]. \tag{28}$$

Note that these potentials are *only* used above $r_c = 3$ fm and thus form factors accounting for the finite size of the nucleon can be set to one. Energy dependence is present through the parameter

$$\alpha' = \alpha\frac{1 + 2k^2/M_p^2}{\sqrt{1 + k^2/M_p^2}}, \tag{29}$$

where k is the center of mass momentum and α the fine structure constant. **Table 1** lists the values used for the fundamental constants in our calculations and typically used since the benchmarking Nijmegen analysis.

3.5. Short Range Contributions

The short range contributions are fundamentally unknown and, despite some lattice QCD efforts [36–38, 44], can only be determined indirectly and phenomenologically, mostly from NN scattering. Along the years some experience has been gathered about the size, shape, and range of the potentials in the bulk, at least in configuration space, so that refinements are made by a χ^2 minimization to pp and np scattering data (see below). Besides, the analysis of scattering data allows to obtain information on

TABLE 1 | Values of fundamental constants used.

Constant	Value	Units
$\hbar c$	197.327053	MeV fm
m_{π^0}	134.9739	MeV/c^2
$m_{\pi^\pm}$	139.5675	MeV/c^2
M_p	938.27231	MeV/c^2
M_n	939.56563	MeV/c^2
m_e	0.510999	MeV/c^2
α^{-1}	137.035989	
f^2	0.075	
μ_p	2.7928474	μ_0
μ_n	−1.9130427	μ_0

the lowest distance where the long range contributions can be trusted. We anticipate that they may be assumed to be valid for $r_c \geq 1.8$ fm when OPE and TPE contributions are included. This coincides *a fortiori* with the distance above which protons interact by Coulomb force as point-like particles, and also with the typical distance between nucleons in nuclear matter, $d = \rho^{-1/3} = 1.8$ fm for $\rho = 0.17\,\text{fm}^{-3}$.

Finally, there is the issue on *which* and *how many* parameters are needed to describe the short range force in a satisfactory manner. The primary 2013 Granada analysis has been carried out in terms of the so-called coarse grained potentials [45]. The coarse grain procedure *samples* the interaction with an optimal grain size, corresponding roughly to the reduced de Broglie wavelength $\Delta r = \hbar/p$. For the maximum LAB energy, 350 MeV, this corresponds to $\Delta r = 0.6$ fm. Thus, we do not need to sample the potential functions $V_i(r)$ at *all* points, but rather in a grid of points, $V_i(r_n)$ given by $r_n = n\Delta r$. We consider the $V_i(r_n)$ values as fitting parameters. The particular interpolations between these points are not physically relevant, because shorter scales than Δr cannot be probed by the scattering process below a maximal $p = \sqrt{T_{\rm LAB} M_N/2} \sim 2\,\text{fm}^{-1}$.

The number of grid points depends on the cut distance, r_c, above which the functional form of the potential is known and corresponds to $N = r_c/\Delta r$. Thus, the simplest case corresponds to $r_c = 1.8$ fm and $N = 3$ grid points for any radial component, $V_i(r_n)$, in the operator basis. In the partial wave basis some refinements can be incorporated since the centrifugal barrier limits the sampling points below the barrier in the classically forbidden region, so that the estimate is Fernandez-Soler and Ruiz Arriola [46] and Ruiz Arriola and Ruiz de Elvira [47],

$$N_{\rm Par} \sim \frac{1}{2}(p_{\rm CM}^{\rm max} r_c)^2\, g_S\, g_T\,, \tag{30}$$

where g_S and g_T are spin and isospin degeneracy factors. The counting of parameters for pp and np [48] yields about 40 "grained" points r_n in the fit carried up to a maximum energy $T_{\rm LAB} \leq 350$ MeV. This *a priori* estimate coincides in the bulk with the number of parameters which have traditionally been needed to fit data satisfactorily in the past. The previous argument suggests that including more parameters is not expected to improve significantly the fits to scattering data, but rather increase the correlations among the $V_i(r_n)$ parameters.

There are many possible ways to describe the interaction at the "grained" points. The simplest is to consider Dirac delta-shells located at the sampled points [49, 50]

$$V(r)|_{\rm Short} = \Delta r \sum_{i,n} O_i V_i(r_n)\delta(r - r_n) \qquad r \leq r_c \tag{31}$$

We refer to Navarro Perez et al. [51] for a pedagogical presentation of coarse grained interactions which solve the Schrödinger equation by a discretized form [49, 50] of the variable phase approach of Calogero [52]. This delta-shells decomposition implies a similar one at the partial waves level, so that one may use the partial wave strengths $V^{JS}_{LL'}(r_n)$ as fitting parameters. This choice is rather convenient for least squares minimization as the low angular momentum partial wave components of the potential are largely uncorrelated, substantially speeding up the minimum search [53, 54]. The transformation matrix from the $V_i(r_n)$ to the $V^{JS}_{LL'}(r_n)$ basis can be found in Navarro Pérez et al. [42].

4. PARTIAL WAVE ANALYSIS

The NN scattering amplitude has five independent complex components which are a function of energy and scattering angle [55],

$$\begin{aligned} M =& a + m(\sigma_1\cdot\mathbf{n})(\sigma_2\cdot\mathbf{n}) + (g-h)(\sigma_1\cdot\mathbf{m})(\sigma_2\cdot\mathbf{m}) \\ &+(g+h)(\sigma_1\cdot\mathbf{l})(\sigma_2\cdot\mathbf{l}) + c(\sigma_1+\sigma_2)\cdot\mathbf{n}. \end{aligned} \tag{32}$$

We use the three unit vectors ($\mathbf{k}_f$ and $\mathbf{k}_i$ are relative final and initial momenta),

$$\mathbf{l} = \frac{\mathbf{k}_f + \mathbf{k}_i}{|\mathbf{k}_f + \mathbf{k}_i|}\,, \qquad \mathbf{m} = \frac{\mathbf{k}_f - \mathbf{k}_i}{|\mathbf{k}_f - \mathbf{k}_i|}\,, \qquad \mathbf{n} = \frac{\mathbf{k}_f \wedge \mathbf{k}_i}{|\mathbf{k}_f \wedge \mathbf{k}_i|}\,. \tag{33}$$

For this amplitude the total spin S is conserved and in this case the partial wave expansion reads,

$$\begin{aligned} M^s_{m'_s,m_s}(\theta) =& \frac{1}{2ik}\sum_{J,l',l}\sqrt{4\pi(2l+1)}\,Y^{l'}_{m'_s-m_s}(\theta,0) \\ &\times C^{l',S,J}_{m_s-m'_s,m'_s,m_s}\, i^{l-l'}(\mathbf{S}^{J,S}_{l,l'} - \delta_{l',l})C^{l,S,J}_{0,m_s,m_s}, \end{aligned} \tag{34}$$

where $\mathbf{S}$ is the unitary coupled channel S-matrix, and the $C's$ are Clebsch-Gordan coefficients, $C^{l,S,J}_{m,m_s,M} = \langle lmSM_s|JM\rangle$. The spins of the nucleon pair can be coupled to total spin $S = 0, 1$ and hence $J = L \pm 1$ for unnatural parity, $(-1)^{L+1}$ states and $J = L$ for natural parity states. This amplitudes contains all measurable physical information and the relation to observable quantities such as differential cross sections and polarization asymmetries can be found in Hoshizaki [56] and Bystricky et al. [57].

In the Stapp-Ypsilantis-Metropolis (SYM) representation [4] the S-matrix is written in terms of the *nuclear-bar phase shifts* $\bar\delta_{j\pm1}$ and $\bar\epsilon_j$. Dropping the bars for simplicity and denoting the phase shifts as $\delta^{J,s}_{l,l'}$, for the singlet ($s = 0, l = l' = J$) and triplet uncoupled ($s = 1, l = l' = J$) channels the S matrix is simply

$e^{2i\delta^{J,s}_{l,l}}$, in the triplet coupled channel ($s=1, l=J\pm 1, l'=J\pm 1$) it reads

$$S^J = \begin{pmatrix} e^{2i\delta^{J,1}_{J-1}}\cos 2\epsilon_J & ie^{i(\delta^{J,1}_{J-1}+\delta^{J,1}_{J+1})}\sin 2\epsilon_J \\ ie^{i(\delta^{J,1}_{J-1}+\delta^{J,1}_{J+1})}\sin 2\epsilon_J & e^{2i\delta^{J,1}_{J+1}}\cos 2\epsilon_J \end{pmatrix}, \tag{35}$$

with ϵ_J the mixing angle.

The partial wave expansion provides an indirect way to find out the range of nuclear forces by truncating the expansion. According to the standard semi-classical argument (see e.g., [58]), for an impact parameter $b=(J+1/2)/p$ (p is the CM momentum) the no-scattering condition corresponds to $b \geq a$, so that $|\delta_{J_{\max}}| \leq \Delta\delta_{J_{\max}}$ where maximal angular momentum is provided by $J_{\max} \approx pa$ with a the range of the force. For the Yukawa OPE interaction the exponential fall-off of the potential also means a similar behavior for the phase-shifts, so typically one takes S, P, D, and F waves as *active* if the condition is $J+1/2 \approx pr_c$ with r_c the separation distance.

We will review briefly the basics of scattering from a NN potential for completeness and to provide our notation. Details may be found in standard textbooks on scattering theory (see e.g., [59]). The generalization of the well-known Rayleigh expansion for spin S is

$$e^{i\mathbf{k}\cdot\mathbf{x}}\chi_{SM_s} = 4\pi\sum_{l,m} i^l j_l(kr) Y^*_{l,m}(\hat{\mathbf{k}}) \sum_{J,M}\langle lmSM_s|JM\rangle \mathcal{Y}_{lSJM}(\hat{\mathbf{x}}), \tag{36}$$

where χ_{SM_s} is an eigenspinor with spin quantum numbers (S, M_s), and the functions $\mathcal{Y}_{lSJM}(\hat{\mathbf{x}})$ are the couplings of the spherical harmonics with the spinors χ_{SM_s} to total angular momentum J,

$$\mathcal{Y}_{lSJM}(\hat{\mathbf{x}}) = \sum_{m',M'_s}\langle lm'SM'_s|JM\rangle Y_{l,m'}(\hat{\mathbf{x}})\,\chi_{SM'_s}\,. \tag{37}$$

The local (but angular momentum dependent) NN potential described in the previous section conserves spin S and total angular momentum J, but not the orbital angular momentum L. Therefore, the scattering wave function for spin S is expanded as

$$\Psi_{\mathbf{k},SM_s}(\mathbf{x}) = 4\pi\sum_{lmJM} i^l Y^*_{l,m}(\hat{\mathbf{k}})\langle lmSM_s|JM\rangle \sum_{l'}\frac{u^{SJ}_{l'l}(r)}{kr}\mathcal{Y}_{l'SJM}(\hat{\mathbf{x}})\,. \tag{38}$$

where the reduced radial wave functions $u^{SJ}_{l'l}(r)$ satisfy the coupled channel differential equations

$$\left[-\frac{d^2}{dr^2}+\frac{l'(l'+1)}{r^2}-k^2\right]u^{SJ}_{l'l} + \sum_{l''}U^{SJ}_{l',l''}(r)u^{SJ}_{l''l} = 0 \tag{39}$$

and the reduced potential is defined as $U(r)=2\mu V(r)$. For regular potentials the boundary condition at the origin reads

$$u^{SJ}_{l'l}(r) \sim r^{l'+1} \qquad (r\to 0) \tag{40}$$

The integration of the equations can advantageously be done using the delta shell representation of the NN potential taking $\Delta r = 0.6$ fm for $r \leq r_c$ (the coarse-grained and unknown part) and $\Delta r = 0.1$ fm for $r \geq r_c$ (the known field theoretical part). The complete set of equations including Coulomb forces is provided in Navarro Pérez et al. [42]. The scattering boundary condition

$$\Psi_{S,m_s}(\vec{x}) \to e^{i\vec{k}\cdot\vec{x}}\chi_{S,m_s} + \frac{e^{ikr}}{r}\sum_{m_{s'}=-S}^{S} M_{m_S,m_{S'}}\chi_{S,m'_s} \tag{41}$$

implies a similar asymptotic condition for the reduced radial wave functions. For the uncoupled case, $l=J$, one has for $r\sim R \gg 1/m_\pi$

$$u_J(r) \equiv u_{JJ}(r) \to \hat{j}_J(kr) - \cot\delta_J(k)\hat{y}_J(kr) \tag{42}$$

where $\hat{j}_J(x)=xj_J(x)$ and $\hat{y}_J(x)=xy_J(x)$ are the reduced spherical Bessel functions of order J and $\delta_J=\delta^{1J}_J, \delta^{0J}_J$. In the coupled triplet case, $S=1$, the four wave functions $u_{l'l}(r)$, with $l', l = J-1, J+1$, are coupled in pairs. The pair

$$v_{\alpha J} = u_{J-1,J-1} \qquad w_{\alpha J} = u_{J+1,J-1} \tag{43}$$

verifies the coupled equations

$$\left[-\frac{d^2}{dr^2}+\frac{J(J-1)}{r^2}-k^2\right]v_{\alpha J} + U^{SJ}_{J-1,J-1}(r)v_{\alpha J} + U^{SJ}_{J-1,J+1}(r)w_{\alpha J} = 0 \tag{44}$$

$$\left[-\frac{d^2}{dr^2}+\frac{(J+1)(J+2)}{r^2}-k^2\right]w_{\alpha J} + U^{SJ}_{J+1,J+1}(r)w_{\alpha J} + U^{SJ}_{J+1,J-1}(r)v_{\alpha J} = 0 \tag{45}$$

On the other hand the pair

$$w_{\beta J} = u_{J+1,J+1} \qquad v_{\beta J} = u_{J-1,J+1} \tag{46}$$

verifies the same coupled equations by changing $\alpha \to \beta$. This is equivalent to say that the system (44, 45) has two linearly independent solutions that we label as α and β solutions. Their asymptotic behavior can be expressed in terms of the eigen phase shifts as,

$$v_{\alpha J}(r) \to \hat{j}_{J-1}(kr)\cot\delta^{1J}_{J-1} - \hat{y}_{j-1}(kr) \tag{47}$$

$$w_{\alpha J}(r) \to \tan\epsilon_J\left[\hat{j}_{j+1}(kr)\cot\delta^{1J}_{J-1} - \hat{y}_{j+1}(kr)\right] \tag{48}$$

$$v_{\beta J}(r) \to -\tan\epsilon\left[\hat{j}_{j-1}(kr)\cot\delta^{1J}_{J+1} - \hat{y}_{j-1}(kr)\right] \tag{49}$$

$$w_{\beta J}(r) \to \hat{j}_{j+1}(kr)\cot\delta^{1J}_{J+1} - \hat{y}_{j+1}(kr) \tag{50}$$

This is known as the Blatt-Biedenharn (BB) parameterization in terms of the *eigen phase shifts* $\delta^{1j}_{j\pm1}$ and ϵ_j. These are related to the nuclear-bar phase shifts by the following equations

$$\delta^{1J}_{J-1} + \delta^{1J}_{J+1} = \bar{\delta}^{1J}_{J-1} + \bar{\delta}^{1J}_{J+1} \tag{51}$$

$$\sin(\bar{\delta}^{1J}_{J-1} - \bar{\delta}^{1J}_{J+1}) = \frac{\tan 2\bar{\epsilon}_J}{\tan 2\epsilon_J} \tag{52}$$

$$\sin(\delta^{1J}_{J-1} - \delta^{1J}_{J+1}) = \frac{\sin 2\bar{\epsilon}_J}{\sin 2\epsilon_J} \tag{53}$$

Unless otherwise stated, in this work the phase shifts will always be assumed to be the nuclear-bar ones. The Coulomb force is included exactly by replacing in the previous formulas the Bessel functions j_l and y_l by Coulomb functions F_l and G_l [59]. The inclusion of magnetic moments effect is complicated by their $1/r^3$ behavior requiring about 1,000 partial waves [42].

5. STATISTICS

The statistical treatment we follow here is quite standard, and we list for the benefit of the newcomer to the field the main steps to be discussed in the following subsections. We first address the existing scattering data and then we formulate the nature of the problem and the standard χ^2 approach searching for the most likely potential. This requires discriminating between consistent and inconsistent data, something which can be formulated in terms of a self-consistent selection problem. After this, a direct statistically satisfactory result can be deduced and, more importantly, error propagation may legitimately be carried out in terms of the corresponding covariance matrix implementing statistical correlations. This allows in particular to determine the scattering phase-shifts with error bars reflecting directly the experimental uncertainties. More generally, it allows to transport these experimental errors to any observable based on the nucleon-nucleon potential. We will call these the statistical errors.

5.1. Scattering Data

Once we have defined the potential model and the scattering formalism we may proceed to determine the potential parameters $V_i(r_n)$ from the available np and pp scattering data and from the corresponding scattering observables which are obtained from the scattering amplitude [56, 57] (see also **Tables 2**, **3** below for the notation). The compilation of the existing published data since 1950 till 2013 is described in detail in Navarro Pérez et al. [42] and comprises 8,124 fitting data including 7,709 experimental measurements and 415 normalizations provided by the experimentalists.

5.2. Statement of the Problem

The finite amount, precision and limited energy range of the data as well as the many different observables calls for a standard statistical χ^2-fit analysis [62, 63]. This approach is subjected to assumptions and applicability conditions that can only be checked *a posteriori* in order to guarantee the self-consistency of the analysis. Indeed, scattering experiments deal with counting Poisson statistics and for moderately large number of counts a normal distribution is expected. Thus, one hopes that a satisfactory theoretical description $O_i^{\rm th}$ can predict a set of N independent observed data O_i given an experimental uncertainty ΔO_i as

$$O_i = O_i^{\rm th} + \xi_i \Delta O_i \tag{54}$$

TABLE 2 | Contributions to the total χ^2 for different pp observables [60, 61].

Observable	Code	N_{pp}	χ^2_{pp}	χ^2_{pp}/N_{pp}
$d\sigma/d\Omega$	DSG	935	903.5	0.97
A_{yy}	AYY	312	339.0	1.09
D	D	104	135.1	1.30
P	P	807	832.4	1.03
A_{zz}	AZZ	51	47.4	0.93
R	R	110	112.8	1.03
A	A	79	70.5	0.89
A_{xx}	AXX	271	250.7	0.92
C_{kp}	CKP	2	3.1	1.57
R'	RP	29	11.9	0.41
$M_{s'0sn}$	MSSN	18	13.1	0.73
$N_{s'0kn}$	MSKN	18	8.5	0.47
A_{zx}	AZX	264	250.6	0.95
A'	AP	6	0.8	0.14

We use the notation of Hoshizaki [56] and Bystricky et al. [57].

TABLE 3 | Contributions to the total χ^2 for different np observables [60, 61].

Observable	Code	N_{np}	χ^2_{np}	χ^2_{np}/N_{np}
$d\sigma/d\Omega$	DSG	1712	1803.4	1.05
D_t	DT	88	83.7	0.95
A_{yy}	AYY	119	96.0	0.81
D	D	29	37.1	1.28
P	P	977	941.7	0.96
A_{zz}	AZZ	89	108.1	1.21
R	R	5	4.5	0.91
R_t	RT	76	72.2	0.95
R'_t	RPT	4	1.4	0.35
A_t	AT	75	77.0	1.03
$D_{0s''0k}$	D0SK	29	44.0	1.52
$N_{0s''kn}$	NSKN	29	25.5	0.88
$N_{0s''sn}$	NSSN	30	20.3	0.68
N_{0nkk}	NNKK	18	13.5	0.75
A	A	6	2.9	0.49
σ	SGT	411	500.2	1.22
$\Delta\sigma_T$	SGTT	20	26.3	1.31
$\Delta\sigma_L$	SGTL	16	18.4	1.15

We use the notation of Hoshizaki [56] and Bystricky et al. [57].

with $i = 1, \ldots, N$ and ξ_i are independent random *normal* variables with vanishing mean value $\langle \xi_i \rangle = 0$ and unit variance $\langle \xi_i \xi_j \rangle = \delta_{ij}$, implying that $\langle O_i \rangle = O_i^{\rm th}$. Establishing the validity of Equation (54) is of utmost importance since it provides a basis for the statistical interpretation of the error analysis.

5.3. The Least Squares Minimization

If the ξ_i are independent normal variables,then $\sum_{i=1}^{\nu} \xi_i^2$ represents a χ^2 distribution with ν degrees of freedom. Thus, under this *hypothesis* we may consider the standard χ^2 method,

which in our case is defined as

$$\chi^2[V_k(r_n)] = \sum_{i=1}^{N_{\rm Dat}} \left[\frac{O_i^{\rm exp} - O_i^{\rm th}(V_k(r_n))}{\Delta O_i^{\rm exp}} \right]^2 \tag{55}$$

where $O_i^{\rm exp}$ is the experimental observable, $\Delta O_i^{\rm exp}$ its estimated uncertainty and $O_i^{\rm th}(V_k(r_n))$ are the theoretical results which depend on the fitting parameters $V_k(r_n)$, the values of the potentials at the sampled points r_n. The least squares minimization has always a solution which may be a global or a local minimum, namely

$$\chi^2_{\rm min} = \min_{V_k(r_n)} \chi^2[V_k(r_n)] \equiv \chi^2[\bar{V}_k(r_n)] \tag{56}$$

where $\bar{V}_k(r_n)$ the minimizing parameters. Basically, this minimization eliminates $N_{\rm Par}$ parameters from the $N_{\rm Dat}$ data and we are left with $\nu = N_{\rm Dat} - N_{\rm Par}$ degrees of freedom. The important aspect here is the *statistical significance* of the procedure. This can be checked *a posteriori* by looking at the residuals

$$R_i = \frac{O_i^{\rm exp} - O_i^{\rm th}|_{\rm min}}{\Delta O_i^{\rm exp}} \tag{57}$$

where $O_i^{\rm th}|_{\rm min} = O_i^{\rm th}(\bar{V}_k(r_n))$. According to the assumption underlying the χ^2-method, the set of variables $R_1, \ldots, R_{N_{\rm par}}$ should be distributed as normal variables, i.e., they should look as $N_{\rm Par}$ variables extracted from a normal distribution $N(0,1)$. For a finite sample the veracity of this hypothesis can only be established in probabilistic terms, so that we may estimate how likely or unlikely would it be to accept of reject the starting normality assumption. Technically, this can be done in a variety of ways (see e.g., [53, 54, 64]), but the most popular measure of goodness of a fit is the χ^2-test which requires that the fit is accepted if

$$\frac{\chi^2_{\rm min}}{\nu} = 1 \pm \sqrt{\frac{2}{\nu}} \tag{58}$$

with $\nu = N_{\rm Dat} - N_{\rm Par}$. More elaborate tests may be applied and we refer to Navarro Perez et al. [53, 54, 64] for further details. In practice this means that for $N_{\rm Dat} = 8000$ and $N_{\rm Par} = 50$ we should get $\chi^2_{\rm min}/\nu = 1 \pm 0.016$ in order to validate Equation (54). Note that this is *very different* than the loose claims in the literature where $\chi^2/\nu \approx 1$ qualifies for a good fit, complemented with a visual inspection of the phase shifts. We emphasize that *looking similar* is not the same as *statistical consistency*. In fact, a direct fit to the full database with our model gives $\chi^2_{\rm min}/\nu = 1.41$ which is 25σ away from the expected value. This clearly indicates either a bad model, inconsistent data, or both. A statistical measure of the probability that the theory is plausible is given by the p-value; assuming that the normality of residuals is correct it corresponds to the probability of obtaining results at least as extreme as the results actually observed [62, 63]. Thus, the probability of having $\chi^2_{\rm min}/\nu = 1.41$ for $\nu \sim 7000$ is $p = 10^{-20}$, which clearly rules out that the theory describes the data within fluctuations.

5.4. Inconsistent vs. Consistent Data

The determination of theoretical uncertainties requires as a prerequisite the compatibility or consistency of all data. This is a strong condition which is not always fulfilled, particularly when the number of data becomes large. Most often, different experiments have different sources of errors and are mutually incompatible. Thus, while any statistical analysis benefits from a large amount of data, a side effect is the proliferation of inconsistent data. In that case it is obvious that no model will be able to simultaneously describe all the data in a satisfactory manner. To appreciate this point more clearly, assume two experiments which yield the measurements $O_{\rm exp1} \pm \Delta O_{\rm exp1}$ and $O_{\rm exp2} \pm \Delta O_{\rm exp2}$. If the theoretical estimate is $O_{\rm th}$, we have

$$\chi^2 = \left[\frac{O_{\rm exp1} - O_{\rm th}}{\Delta O_{\rm exp1}} \right]^2 + \left[\frac{O_{\rm exp2} - O_{\rm th}}{\Delta O_{\rm exp2}} \right]^2 \tag{59}$$

Minimizing respect to $O_{\rm th}$ we get

$$\chi^2_{\rm min} = \frac{(O_{\rm exp1} - O_{\rm exp2})^2}{\Delta O^2_{\rm exp1} + \Delta O^2_{\rm exp2}} \tag{60}$$

which becomes larger than 1 for $|O_{\rm exp1} - O_{\rm exp2}| \geq \sqrt{\Delta O^2_{\rm exp1} + \Delta O^2_{\rm exp2}}$, in which case we have two *inconsistent* measurements. The important question is whether both measurements are wrong or just only one. The term wrong here does not necessarily mean an incorrect measurement; it suffices if *one* or *both* errors $\Delta O_{\rm exp1}$ and $\Delta O_{\rm exp2}$ are unrealistically small. In case of a discrepancy one may re-analyze the experiment or simply ask the experts, an unfeasible strategy for the experiments performed in the time span 1950–2013 comprising the analysis. The advantage of the statistical method is that, for a large number of experiments, the systematic errors are also randomized and one may rule out some experiments in a kind of majority vote argument.

The case discussed previously corresponds to two different measurements of the *same* observable, say the differential cross section at the same energy and angle, and the generalization to any number of experiments is straightforward. However, in the case of experiments with close kinematics there is no simple way to decide between inconsistent data unless some continuity and smooth behavior is assumed in order to intertwine the two measurements. Here is where the *model* enters and statistical methods will never tell us if a given model is correct but rather if the model is inconsistent with the data. This is a kind of circular argument which can only be avoided by looking for models which congregate as many data as possible in a consistent way. Clearly, following this criterion, once one finds a good model, any improvement of the model should describe *more data* in a statistically significant fashion. The great advantage is that if there are reasons to intertwine theoretically the different measurements of all possible observables one may discuss the data consistency in a generalized way and be able to select between different observables.

5.5. Self-Consistent Data Selection

The self-consistent criterion for data selection was proposed by Gross and Stadler [19] and implemented in Navarro Pérez et al. [45]. The way data have been selected proceeds according to the following procedure:

1. Fit the model to all data. If $\chi^2/\nu < 1$ you can stop. If not proceed further.
2. Remove data sets with improbably high or low χ^2 (3σ criterion).
3. Refit parameters for the remaining data.
4. Re-apply 3σ criterion to all data.
5. Repeat until no more data are excluded or recovered.

The effect of the selection criterion with our model is to go from $\chi^2/\nu|_{\rm all} = 1.41$ to $\chi^2/\nu|_{\rm selected} = 1.05$ with a reduction in the number of data from $N_{\rm Data} = 8173$ to $N_{\rm Data} = 6713$. While this seems a drastic rejection it is the largest self-consistent fit to date below 350 MeV. For this number of data this is *not* a minor improvement; in terms of a normality test, it makes the difference in p-value between having $p = 10^{-20}$ or $p = 0.68$.

5.6. Fitting Results

The set of 32 scattering observables which we use for the fits comprises a total of about 7000 selected measurements. It is interesting to decompose the contributions to the total χ^2 both in terms of the fitted observables as well as in different energy bins. The separation is carried out explicitly in **Tables 2**, **3** for pp and np scattering observables respectively and for the latest fit which includes also the pion-nucleon coupling constants [60, 61] (see below). As we can see the size of the contributions χ^2/N are at similar levels for most observables. Note that observables with a considerable larger or smaller χ^2/N are also observables with a small number of data and therefore larger statistical fluctuations are expected (we remind that for N *independent data* we expect $\chi^2/N \approx 1 \pm \sqrt{2/N}$.

Likewise, we can also break up the contributions in order to see the significance of different energy intervals, see **Table 4**. We find that, in agreement with the Nijmegen analysis (see [65, 66] for comparisons with previous potentials), there is a relatively large degree of uniformity in describing data at different energy bins. We note also that the fit in the low energy region below 2 MeV gives the largest values for χ^2/N.

From the optimal fitting parameters $V^\alpha(r_n)$ with $\alpha = {}^1S_0, {}^3P_0, {}^3S_1, {}^3D_1, E_1, \ldots$ being the different partial waves in a given pp or np channel, we define $(\lambda_n)^\alpha = 2\mu_{ab} V^\alpha(r_n)\Delta r$ which has units of fm^{-1} and $ab = pp, np$. In **Table 5** we show the corresponding numerical values. It would be nice to see whether something can be said about the nn interaction. However, one remarkable feature of this and similar analyses is the fact that with the exception of S-waves the short distance parameters can be chosen to coincide in the pp and np systems with common partial waves. The fact that to this date it is not possible to do it for S-waves precludes to predict the nn interaction from the combined *np* and *pp* fit (see however a theoretical discussion in Calle Cordon et al. [67]).

TABLE 4 | The χ^2 results of the main combined *pp* and *np* partial-wave analysis [60, 61] for the 10 single-energy bins in the range $0 < T_{\rm LAB} < 350$ MeV.

Bin (MeV)	N_{pp}	χ^2_{pp}	χ^2_{pp}/N_{pp}	N_{np}	χ^2_{np}	χ^2_{np}/N_{np}	N	χ^2	$\chi^2/N\|_{\rm fit}$	$\chi^2/N\|_{\rm th}$
0.0–0.5	103	107.2	1.04	46	88.2	1.92	149	195.4	1.31	1 ± 0.11
0.5–2	82	58.8	0.72	50	92.8	1.86	132	151.5	1.15	1 ± 0.12
2–8	92	80.1	0.87	122	151.0	1.24	214	231.0	1.08	1 ± 0.10
8–17	124	100.3	0.81	229	183.9	0.80	353	284.1	0.80	1 ± 0.08
17–35	111	85.5	0.77	346	324.2	0.94	457	409.7	0.90	1 ± 0.07
35–75	261	231.2	0.89	513	559.7	1.09	774	790.9	1.02	1 ± 0.05
75–125	152	154.8	1.02	399	445.2	1.12	551	600.0	1.09	1 ± 0.06
125–183	301	300.5	1.00	372	381.7	1.03	673	682.2	1.01	1 ± 0.05
183–290	882	905.0	1.03	858	841.4	0.98	1740	1746.4	1.00	1 ± 0.03
290–350	898	956.1	1.06	798	808.1	1.01	1696	1764.1	1.04	1 ± 0.03

We compare the fit $\chi^2/N|_{fit}$ with the theoretical expectation $\chi^2/N|_{th} = 1 \pm \sqrt{2/N}$.

TABLE 5 | Fitting delta-shell parameters $(\lambda_n)^{JS}_{l,l'}$ (in fm^{-1}) with their errors for all states in the *JS* channel for a fit with isospin symmetry breaking on the $^1S_0$ partial wave parameters only and the pion-nucleon coupling constants f_0^2, f_p^2, and f_c^2 as fitting parameters We take $N = 5$ equidistant points with $\Delta r = 0.6$ fm.

Wave	λ_1	λ_2	λ_3	λ_4	λ_5
$^1S_{0np}$	1.16(6)	-0.77(2)	-0.15(1)	–	-0.024(1)
$^1S_{0pp}$	1.31(2)	-0.716(5)	-0.192(2)	–	-0.0205(4)
$^3P_0$	–	0.94(2)	-0.319(7)	-0.062(3)	-0.023(1)
$^1P_1$	–	1.20(2)	–	0.075(2)	–
$^3P_1$	–	1.354(5)	–	0.0570(5)	–
$^3S_1$	1.79(7)	-0.47(1)	–	-0.072(2)	–
ε_1	–	-1.65(2)	-0.33(2)	-0.233(7)	-0.018(3)
$^3D_1$	–	–	0.40(1)	0.070(9)	0.021(3)
$^1D_2$	–	-0.20(1)	-0.206(3)	–	-0.0187(3)
$^3D_2$	–	-1.01(3)	-0.17(2)	-0.237(6)	-0.016(2)
$^3P_2$	–	-0.482(1)	–	-0.0289(7)	-0.0037(4)
ε_2	–	0.32(2)	0.190(4)	0.050(2)	0.0127(6)
$^3F_2$	–	3.50(6)	-0.229(5)	–	-0.0140(5)
$^1F_3$	–	–	0.12(2)	0.089(8)	–
$^3D_3$	–	0.54(2)	–	–	–

$f_{\rm p}^2$	f_0^2	$f_{\rm c}^2$
0.0764(4)	0.0779(8)	0.0758(4)

– indicates that the corresponding fitting $(\lambda_n)^{JS}_{l,l'} = 0$. The lowest part of the table shows the resulting OPE coupling constants with errors.

5.7. Covariance Matrix Error Analysis and Statistical Correlations

After the data selection and fitting, error propagation becomes applicable. Here we show the results for the conventional covariance error analysis which assumes small errors and where one first determines the uncertainty in the fitting parameters $V_i(r_n)$ which will be labeled generically as λ_i for ease of notation[2].

[2]The bootstrap approach based on the MonteCarlo method [45, 68] will be discussed below.

Expanding around the minimum values, $\bar{\lambda}_i$ has

$$\chi^2 = \chi^2_{\rm min} + \sum_{ij=1}^{N_P} (\lambda_i - \bar{\lambda}_i)(\lambda_j - \bar{\lambda}_j)\mathcal{E}^{-1}_{ij} + \cdots \tag{61}$$

where the $N_P \times N_P$ error matrix is defined as the inverse of the Hessian matrix evaluated at the minimum

$$\mathcal{E}^{-1}_{ij} = \frac{1}{2}\frac{\partial^2 \chi^2}{\partial\lambda_i \partial\lambda_j}\Big|_{\lambda_i=\bar{\lambda}_i} \tag{62}$$

The correlation matrix between the fitting parameters λ_i and λ_j is given by

$$\mathcal{C}_{ij} = \frac{\mathcal{E}_{ij}}{\sqrt{\mathcal{E}_{ii}\mathcal{E}_{jj}}} \tag{63}$$

We compute the error of the parameter λ_i as

$$\Delta\lambda_i \equiv \sqrt{\mathcal{E}_{ii}}. \tag{64}$$

Error propagation of an observable depending on the fitting parameters $G = G(\lambda_1, \ldots, \lambda_P)$ is computed as

$$(\Delta G)^2 = \sum_{ij} \frac{\partial G}{\partial\lambda_i}\frac{\partial G}{\partial\lambda_j}\Big|_{\lambda_k=\lambda_{k,0}} \mathcal{E}_{ij}. \tag{65}$$

The correlation matrix, Equation (63), has been evaluated in Navarro Perez et al. [53, 54] where it has been found that for the potentials *in the partial wave basis* $V^{JS}_{l,l'}(r_n)$ the different points r_n are largely correlated within a given partial wave, whereas *different* partial waves are largely uncorrelated. This information allows to substantially speed up the minimum search as movements in the multidimensional space are thus independent and the approaching path to the minimum operates stepwise [53, 54].

5.8. Phase-Shifts

The first useful application of error propagation regards scattering amplitudes and phase shifts. Extensive tables for the selected values $T_{\rm LAB} = 1, 5, 10, 25, 50, 100, 150, 200, 250, 300, 350$ MeV have traditionally been presented since the Nijmegen analysis as representative of the fits. These energy values corresponds to a grid of almost equidistant CM momenta $p = \sqrt{T_{\rm LAB} M_N/2}$ between 0 and 2 fm^{-1}.

For illustration, **Figure 1** compares, for low angular momentum, the phase shifts of the primary PWA in Navarro Pérez et al. [42] from a fit with *fixed* pion coupling constant, f^2 (blue bands), and the most recent ones [60] (red band) from a fit with charge symmetry breaking on the $^3P_0$, $^3P_1$, and $^3P_2$ partial waves *and* in the pion coupling constants f_0^2, f_p^2, and f_c^2.

6. DETERMINATION OF YUKAWA COUPLING CONSTANTS

The first determination of the coupling constant was carried out in 1940 by Bethe who obtained the value $f^2 = 0.077 - 0.080$ from the study of deuteron properties [3] and very close to the currently accepted value (see **Table 1**). Subsequent determinations based on a variety of processes can be traced from recent compilations [69, 70]. A recent historical account has been given by Matsinos [71] where some newer determinations can be consulted according to his own eligibility criterium. For completeness we also quote recent studies based on pion-deuteron scattering [72, 73] or on the analysis of Roy equations for πN [74] where an upgrade of the corresponding scattering data is considered.

We note that what follows is a brief summary of the results presented in our previous papers where many more details may be found regarding the most influential observables, the dependence on the cut-off radius r_c, the inclusion of two-pion exchange contributions or the energy range used in the fit or the evolution with the numerical values and precision along the years [60, 61].

The πNN coupling constant is defined as the pion-nucleon-nucleon vertex when the three particles are on the mass shell. The corresponding potentials would be

$$V_{pp\to pp}(r) = f^2_{\pi^0 pp} V_{m_{\pi^0}}(r), \tag{66}$$

$$V_{np\to np}(r) = V_{pn\to pn}(r) = -f_{\pi^0 nn} f_{\pi^0 pp} V_{m_{\pi^0}}(r) \tag{67}$$

$$V_{pn\to np}(r) = V_{np\to pn}(r) = f_{\pi^- pn} f_{\pi^+ np}\, V_{m_{\pi^\pm}}(r) \tag{68}$$

$$V_{nn\to nn}(r) = f^2_{\pi^0 nn} V_{m_{\pi^0}}(r), \tag{69}$$

There exist four pion nucleon coupling constants, $f_{\pi^0 pp}$, $-f_{\pi^0 nn}$, $f_{\pi^+ pn}/\sqrt{2}$, and $f_{\pi^- np}/\sqrt{2}$ which coincide with f when up and down quark masses are identical and the electron charge is zero. In NN interactions we have access to the combinations,

$$\begin{aligned} f_n^2 &= f_{\pi^0 nn} f_{\pi^0 nn}, \\ f_p^2 &= f_{\pi^0 pp} f_{\pi^0 pp}, \\ f_0^2 &= -f_{\pi^0 nn} f_{\pi^0 pp}, \\ 2f_c^2 &= f_{\pi^- pn} f_{\pi^+ np}. \end{aligned} \tag{70}$$

While there is no reason why the pion-nucleon-nucleon coupling constants should be identical in the real world, one expects that the small differences might be pinned down from a sufficiently large number of independent and mutually consistent data. Note that from np and pp analysis we would obtain f_p^2, f_0^2, and f_c^2 we may deduce the nn coupling using the previous equations $f_n = -f_0^2/f_p$. We try to find out how many data would be needed by recalling that electroweak corrections scale with the fine structure constant $\alpha = 1/137$ and the light quark mass differences. Thus,

$$\frac{\delta g}{g} = \mathcal{O}\left(\alpha, \frac{m_u - m_d}{\Lambda_{\rm QCD}}\right) = \mathcal{O}\left(\alpha, \frac{M_p - M_n}{\Lambda_{\rm QCD}}\right) \tag{71}$$

for the relative change around a mean value. These are naturally at the $1 - 2\%$ level, a small effect. The question is on how many independent measurements N are needed to achieve this desired accuracy. According to the central limit theorem, for N

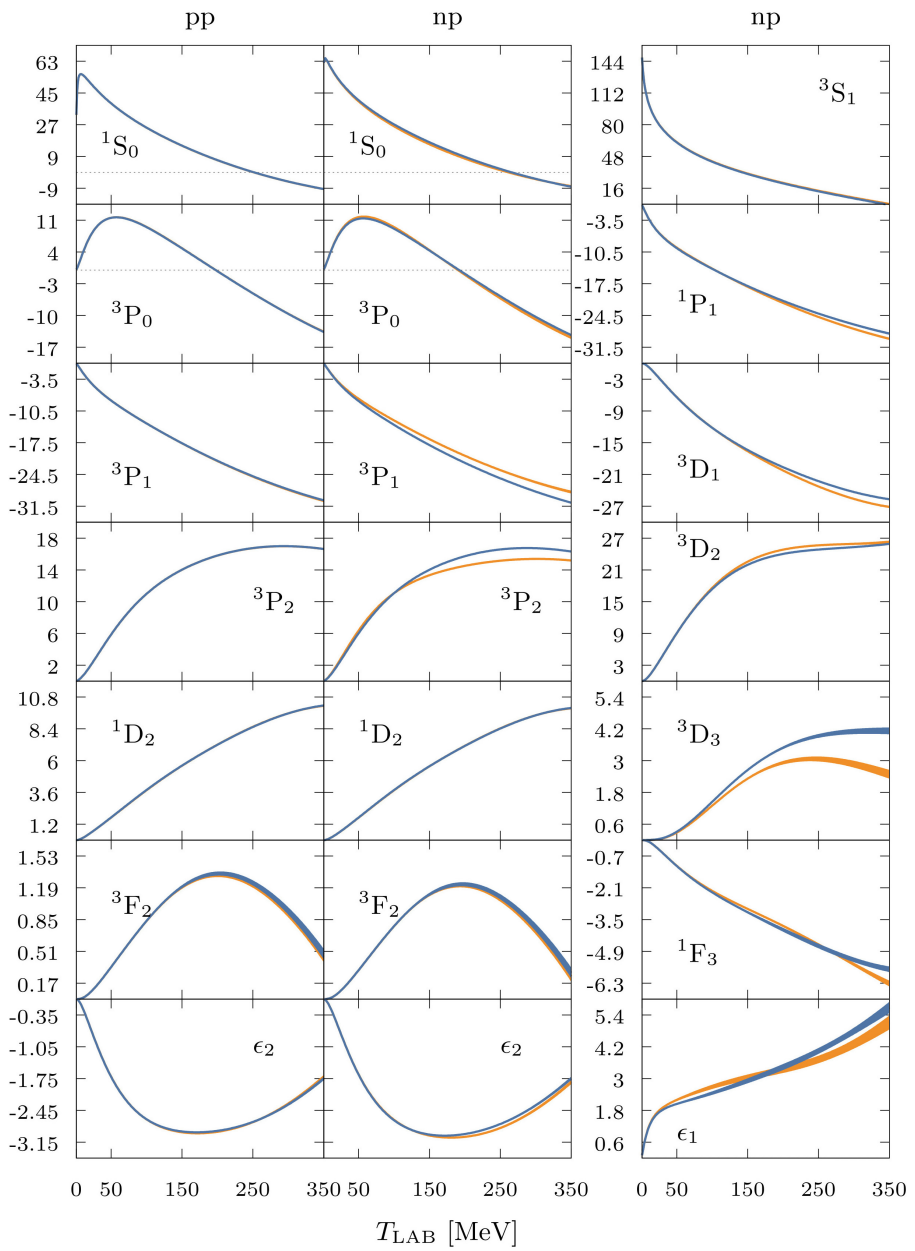

FIGURE 1 | (Color online) Phase shifts obtained from a partial waves analysis to pp and np data and statistical uncertainties. Blue band from Navarro Pérez et al. [42] from a fit with *fixed* f^2 and orange band [60] from a fit with charge symmetry breaking on the $^3P_0$, $^3P_1$, and $^3P_2$ partial waves *and* in the coupling constants f_0^2, f_p^2, and f_c^2.

direct independent measurements the relative standard deviation scales as

$$\frac{\Delta g}{g} = \mathcal{O}\left(\frac{1}{\sqrt{N}}\right)$$

and $\delta g \sim \Delta g$ for $N = 7000 - 10000$. We cannot carry out these direct measurements of g but we can proceed indirectly by considering a set of mutually consistent NN scattering measurements The most recent analysis [60, 61] based on the Granada-2013 database comprises 6713 published data. This allows: (i) to reduce the error bars, as expected and (ii) to discriminate between the three coupling constants (see **Table 6**). When charge dependence in $^1S_0$, P waves is allowed one has

$$f_p^2 = 0.0761(4), \quad f_0^2 = 0.0790(9), \quad f_c^2 = 0.0772(5), \qquad (72)$$

The most remarkable consequence is that from the point of view of the strong interaction neutrons interact more strongly than protons.

7. SYSTEMATIC VS. STATISTICAL ERRORS: THE 6 GRANADA POTENTIALS

Within the phenomenological approach the estimation of systematic errors can be addressed by using different representations of the mid-range function below the separation distance r_c while keeping the long range potential and the NN database. To this end we have analyzed 6 different potentials in Navarro Pérez et al. [75] which have been fitted to the *same* Granada 2013 database and have the *same* long distance components of the potential. First we have checked that the 6 Granada potentials are statistically acceptable. In fact, as it has been stressed in our previous works [53, 54] one can globally slightly enlarge the experimental uncertainties by the so-called Birge factor [76] provided the residuals verify a normality test. After this re-scaling the p-value becomes 0.68 for a 1σ confidence level and hence all potentials become statistically equivalent. The results are summarized in **Table 7**. Thus, the overall spread between the various phenomenological models with $\chi^2/\text{dof} \sim 1$ provides an estimate of the scale of the systematic uncertainty. A direct way of illustrating quantitatively the situation is by analyzing the corresponding phase shifts in the different analyses.

Thus, for each energy and partial wave, one evaluates the phaseshifts $\delta^{(1)}, \ldots, \delta^{(N)}$ for a representative set of high-precision NN potentials $V^{(1)}, \ldots, V^{(N)}$, and computes the average $\overline{\delta}$ and standard deviation

$$\Delta\delta = \text{Std}\,\delta = \sqrt{\frac{1}{N-1}\sum_{i=1}^{N}\left(\delta^{(i)} - \overline{\delta}\right)^2} \tag{73}$$

as a measure of the systematic uncertainty of the phaseshifts. In **Figure 2** we show the results for four different situations. To provide some historical perspective, we show in the upper left panel the averaged phase shifts, i.e., the absolute (mean-square) errors for np partial wave phase shifts due to the different potentials fitting scattering data with $\chi^2/\text{dof} \sim 1$ [15–19] as a function of the LAB energy, namely (CD Bonn) [78], Nijmegen (Nijm-I and Nijm-II) [15], Argonne AV18 [17], Reid (Reid93) [79], and the covariant spectator model [19]. As one naturally expects the average uncertainties grow with energy and decrease with the relative angular momentum which semi-classically corresponds to probing an impact parameter

$$b = \frac{L + 1/2}{p} \tag{74}$$

where p is the CM momentum, $p = \sqrt{M_N E_{\text{LAB}}/2}$, making peripheral waves to be mostly determined from OPE. These analyses stop at the pion production threshold so that one probes distances larger than

$$b_{\min} \sim 1/\Lambda = 0.5\text{fm}, \qquad \Lambda = \sqrt{m_\pi M_N}. \tag{75}$$

Note that the bumps or bulges at low energy in $^1S_0$ and $^3S_1$ channels in the top left panel are due to a unique potential which is an outlier at low energies. In particular, the authors believe that the outlier behavior is due to the use of an interpolating function used to approximate the potential between the values of laboratory energy at which phaseshifts are usually tabulated.

In the upper right panel of **Figure 2** we show the errors obtained via the standard covariance-matrix method explained above and including correlations in the fitting parameters for the primary Granada 2013 analysis [45] which corresponds to the DS-OPE potential. Thirdly, in the lower left panel we show the case of the np phase shifts for the 6 Granada potentials [45, 75, 77]. Finally, in lower right panel we present the uncertainties for all the 7 pre-Granada potentials and the 6 Granada potentials simultaneously.

TABLE 6 | The pion-nucleon coupling constants f_p^2, f_0^2, and f_c^2 determined from different fits to the Granada-2013 database and their characteristics.

f_p^2	f_0^2	f_c^2	CD-waves	χ^2_{pp}	χ^2_{np}	χ^2	N_{Dat}	N_{Par}	χ^2/ν
0.075	Idem	Idem	$^1S_0$	2997.29	3957.57	6954.86	6720	46	1.042
0.0763(1)	Idem	Idem	$^1S_0$	2995.20	3952.85	6947.05	6720	47	1.041
0.0764(4)	0.0779(8)	0.0758(4)	$^1S_0$	2994.41	3950.42	6944.83	6720	49	1.041
0.0761(4)	0.0790(9)	0.0772(5)	$^1S_0$, P	2979.37	3876.13	6855.50	6741	55	1.025

We indicate the partial waves where charge dependence is allowed.

TABLE 7 | Granada potentials summary.

Potential	N_{Par}	N_{np}	N_{pp}	χ^2_{np}	χ^2_{pp}	χ^2/d.o.f.	p-value	Normality	Birge factor
DS-OPE	46	2996	3717	3051.64	3958.08	1.05	0.32	Yes	1.03
DS-χTPE	33	2996	3716	3177.43	4058.28	1.08	0.50	Yes	1.04
DS-ΔBO	31	3001	3718	3396.67	4076.43	1.12	0.24	Yes	1.06
Gauss-OPE	42	2995	3717	3115.16	4048.35	1.07	0.33	Yes	1.04
Gauss-χTPE	31	2995	3717	3177.22	4135.02	1.09	0.23	Yes	1.05
Gauss-ΔBO	30	2995	3717	3349.89	4277.58	1.14	0.20	Yes	1.07

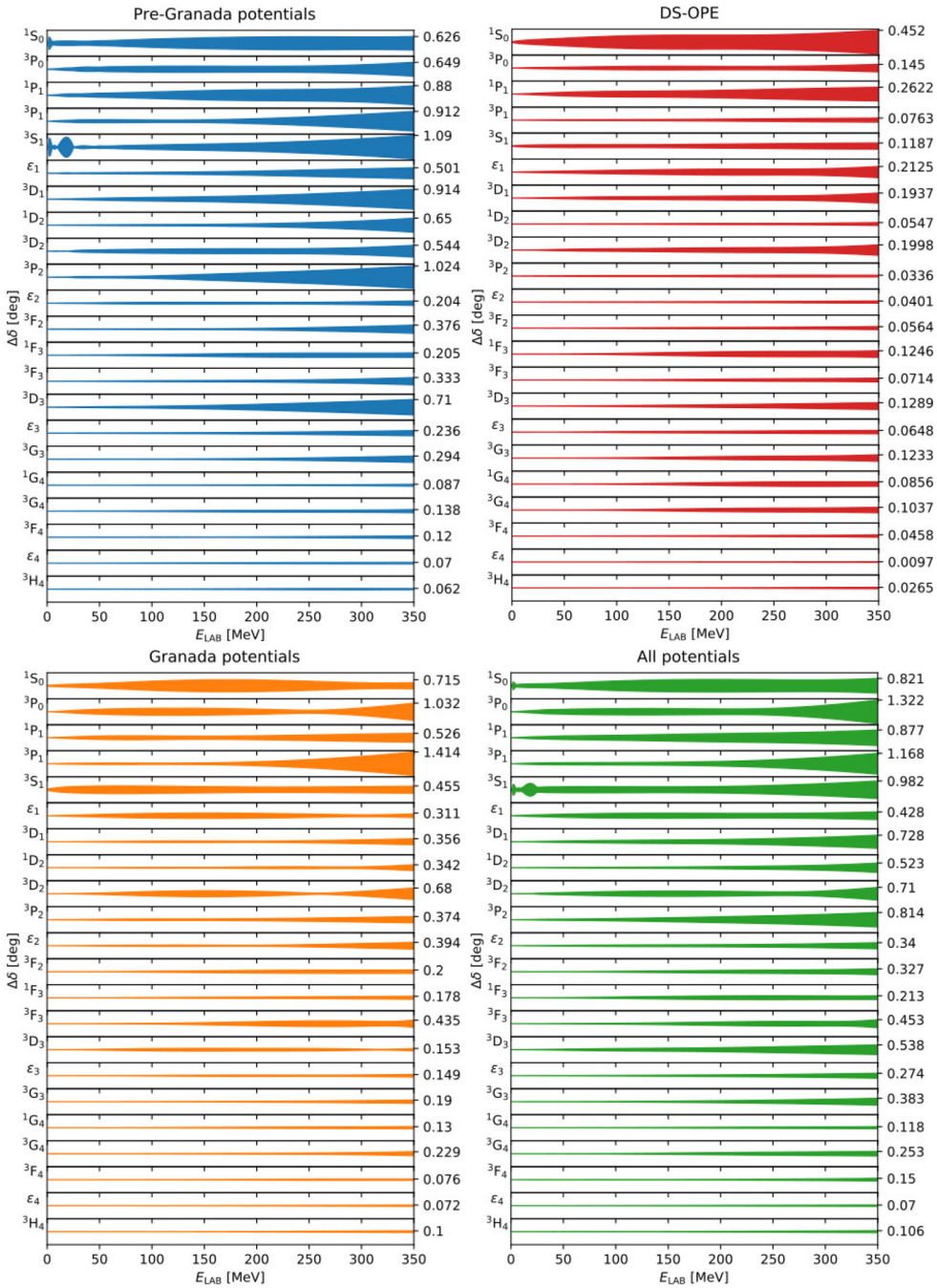

FIGURE 2 | Uncertainties (in degrees, right axis) for partial wave np phase shifts with $J \leq 4$ (left axis) for different potentials fitting scattering data with χ^2/dof ~ 1 as a function of the LAB energy (in MeV). (Upper left) Averaged errors for pre-Granada potentials [15–19]. (Upper right) Statistical errors for the primary Granada 2013 χ^2 analysis [45]. (Lower left) The averaged errors for the 6 Granada potentials [45, 75, 77]. (Lower right) Averaged errors for all 13=7 pre-Granada and the 6 Granada potentials.

In Navarro Pérez et al. [75] we found similar statistical errors in all the Granada potentials, which are statistically validated with the *same* Granada-2013 database, i.e., if the phase-shift for potential $V^{(i)}$ in a given partial wave is $\delta^{(i)} \pm \Delta\delta^{(i)}_{\rm stat}$, then

$$\Delta\delta^{(1)}_{\rm stat} \sim \cdots \sim \Delta\delta^{(6)}_{\rm stat}\,, \tag{76}$$

However, we also found that the standard deviation of systematic errors obeys

$$\Delta\delta_{\rm sys} \equiv {\rm Std}(\delta^{(1)},\ldots,\delta^{(6)}) \gg \Delta\delta^{(i)}_{\rm stat}\,. \tag{77}$$

In all the potentials, the tails *above* $r = 3$ fm (including CD-OPE and all electromagnetic effects) are the *same*, thus the discrepancies between the potentials at short distances dominate the uncertainties, rather than the np and pp experimental data themselves. This conclusion holds also when all high quality potentials are considered [75]. This counter-intuitive result relies not only on the specific forms of potentials which treat the mid– and short-range behavior of the interaction differently but also on the fact that the fits are mainly done to scattering amplitudes rather than to the phase-shifts themselves.

8. LOW ENERGY BEHAVIOR

8.1. Low Energy Parameters

The effective range expansion was proposed by Bethe [80] in order to provide a model independent characterization of the scattering at low energies where the shape of the potential is largely irrelevant. The extension to higher partial waves reads (see e.g., [81])

$$k^{2l+1}M_l(k) \equiv k^{2l+1}\cot\delta_l(k) = -\frac{1}{\alpha_l}+\frac{1}{2}r_l k^2 + v_{2,l}k^4 + v_{3,l}k^6 + \cdots \tag{78}$$

where α_l is the scattering length, r_l the effective range and $v_{i,l}$ the curvature parameters. In the case of coupled channels due to the tensor force one has that $\mathbf{S}^{JS} = (\mathbf{M}^{JS} - i\mathbf{1})(\mathbf{M}^{JS} + i\mathbf{1})^{-1}$ with $(\mathbf{M}^{JS})^\dagger = \mathbf{M}^{JS}$ a hermitian coupled channel matrix (also known as the K-matrix). At the level of partial waves the multi-pion exchange diagrams generate left hand cuts in the complex s-plane, which arise in addition to the NN elastic right cut and the πNN, $2\pi NN$ etc., pion production cuts. At low energies for $|p| \le m_\pi/2$ we have [82]

$$p^{l+l'+1}M^{JS}_{l,l'}(p) = -(\alpha^{-1})^{JS}_{l,l'} + \frac{1}{2}(r)^{JS}_{l,l'}p^2 + (v)^{JS}_{l,l'}p^4 + \ldots \tag{79}$$

which is the coupled channels effective range expansion. While at lowest orders explicit formulas where available in terms of wave functions, larger order and partial waves become rather cumbersome and no practical formula exists.

Fortunately, the variable S-matrix approach of Calogero [52] offers a unique way to extract low-energy threshold parameters for a given NN potential which was extended to coupled channels [82] and applied to the Reid93 and NijmII potentials up to $J \le 5$. For the 6 Granada potentials these have also been extracted and we have found that the systematic uncertainties are generally at least an order of magnitude larger than statistical uncertainties [75]. In **Table 8** where we provide the low energy parameters for ($J \le 2$).

8.2. Low Energy Constants

Alternatively, one may use effective interactions derived from a low momentum interaction where the coefficients can be identified with the phenomenological counter-terms of chiral effective field theory. To obtain such counter-terms we express the momentum space NN potential in the partial wave basis

$$v^{JS}_{l',l}(p',p) = (4\pi)^2\int_0^\infty dr\, r^2\, j_{l'}(p'r)j_l(pr)V^{JS}_{l'l}(r) \tag{80}$$

and use the Taylor expansion of the spherical Bessel function to get an expansion for the potential in each partial wave. Keeping terms up to fourth order $\mathcal{O}(p^4, p'^4, p^3p', pp'^3, p^2p'^2)$ corresponds to keeping only *S*-, *P*-, and *D*-waves along with *S*-*D* and *P*-*F* mixing parameters. Using the normalization and spectroscopic notation of Epelbaum et al. [84] one gets

$$\begin{aligned}
v^{JS}_{00}(p',p) &= \widetilde{C}^{JS}_{00} + C^{JS}_{00}(p^2+p'^2) + D^{1}_{00\,JS}(p^4+p'^4) + D^{2}_{00\,JS}p^2p'^2 + \cdots\\
v^{JS}_{11}(p',p) &= pp'C^{JS}_{11} + pp'(p^2+p'^2)D^{JS}_{11} + \cdots\\
v^{JS}_{22}(p',p) &= p^2p'^2D^{JS}_{22} + \cdots
\end{aligned}$$

TABLE 8 | Low energy threshold np parameters for all partial waves with $j \le 2$.

Wave	α	r_0	v_2	v_3	v_4
$^1S_0$	−23.735(6)	2.673(9)	−0.50(1)	3.87(2)	−19.6(1)
	−23.735(16)	2.68(3)	−0.48(2)	3.9(1)	−19.6(5)
$^3P_0$	−2.531(6)	3.71(2)	0.93(1)	3.99(3)	−8.11(5)
	−2.5(1)	3.7(4)	0.9(5)	3.9(1)	−8.2(9)
$^1P_1$	2.759(6)	−6.54(2)	−1.84(5)	0.41(2)	8.39(9)
	2.78(3)	−6.46(9)	−1.7(2)	0.5(2)	8.0(3)
$^3P_1$	1.536(1)	−8.50(1)	0.02(1)	−1.05(2)	0.56(1)
	1.52(1)	−8.6(1)	−0.06(7)	−0.9(2)	0.1(5)
$^3S_1$	5.435(2)	1.852(2)	−0.122(3)	1.429(7)	−7.60(3)
	5.42(1)	1.84(1)	−0.14(1)	1.46(3)	−7.7(2)
ϵ_1	1.630(6)	0.400(3)	−0.266(5)	1.47(1)	−7.28(2)
	1.61(2)	0.39(2)	−0.29(3)	1.47(2)	−7.35(9)
$^3D_1$	6.46(1)	−3.540(8)	−3.70(2)	1.14(2)	−2.77(2)
	6.43(4)	−3.57(2)	−3.77(4)	1.11(5)	−2.7(1)
$^1D_2$	−1.376	15.04(2)	16.68(6)	−13.5(1)	35.4(1)
	−1.379(6)	15.00(9)	16.7(2)	−12.9(4)	36.2(14)
$^3D_2$	−7.400(4)	2.858(3)	2.382(9)	−1.04(2)	1.74(2)
	−7.39(1)	2.87(1)	2.41(3)	−0.96(5)	1.75(8)
$^3P_2$	−0.290(2)	−8.19(1)	−6.57(5)	−5.5(2)	−12.2(3)
	−0.288(5)	−8.3(2)	−6.8(7)	−6.1(19)	−12.7(26)
ϵ_2	1.609(1)	−15.68(2)	−24.91(8)	−21.9(3)	−64.1(7)
	1.604(6)	−15.8(2)	−25.2(7)	−23.0(29)	−66.2(69)
$^3F_2$	−0.971	−5.74(2)	−23.26(8)	−79.5(4)	−113.0(16)
	−0.971(5)	−5.7(1)	−23.3(6)	−80.1(33)	−117.2(121)

The central value and statistical *error bars are given on the first line of each partial wave and correspond to the mean and standard deviation of a population of* 1020 *parameters calculated with the Monte Carlo family of potential parameters described in Navarro Pérez et al. [83] using the DS-OPE potential [42, 45]. The second line quotes the systematic uncertainties, the central value and error bars correspond to the mean and standard deviation of the 9 realistic potentials NijmII [16], Reid93 [16], AV18 [17], DS-OPE [42, 45], DS-χTPE [48, 77], Gauss-OPE [53], Gauss-χTPE, DS-ΔBO, and Gauss-ΔBO. For each partial wave we show the scattering length α and the effective range r_0, both in fm$^{l+l'+1}$, as well as the curvature parameters v_2 in fm$^{l+l'+3}$, v_3 in fm$^{l+l'+5}$, and v_4 in fm$^{l+l'+5}$. For the coupled channels we use the nuclear bar representation of the S matrix. Uncertainties smaller than* 10^{-3} *are not quoted.*

$$v_{20}^{JS}(p',p) = p'^2 C_{20}^{JS} + p'^2 p^2 D_{20}^{1\,JS} + p'^4 D_{20}^{2\,JS} + \dots$$
$$v_{31}^{JS}(p',p) = p'^3 p D_{31}^{JS} + \cdots \quad (81)$$

and each counter-term can be expressed as a radial momentum of the NN potential in a specific partial wave. Different methods have been proposed to quantify some of the uncertainties in these quantities [85, 86]. Using the statistical uncertainties method and the corresponding systematic error estimates [87], the results are summarized in **Table 9** for the 6 Granada potentials.

8.3. Scale Dependence and Correlations

While one normally uses a *fixed* value for the maximum energy in the fits (which in most NN studies has been 350 MeV), one may analyze the consequences of varying this fitting energy [88]. Denoting Λ as the (running) maximal momentum it is clear that the fitting potential will change as Λ is varied. Actually, these parameters may be mapped [54] into the so-called counter-terms which characterize the effective theories at small momenta [89]. We determined the two-body Skyrme force parameters arising from the NN interaction as a function of the maximal momentum in the fit. We found general agreement with the so-called $V_{\rm lowk}$ interactions based on high quality potentials after high energy components have been integrated out [90, 91].

In line with our remarks in section 5.7 let us note that, one major outcome of Navarro Pérez et al. [54] has been the fact that the counter-terms corresponding to volume integrals including OPE above 3 fm are weakly correlated, whereas those including OPE+TPE above 1.8 fm have larger but still moderate correlations. Thus, counter-terms in the partial waves basis would be efficient fitting parameters, unlike in the cartesian basis. As we have already discussed, using uncorrelated fitting parameters has the practical consequence of reducing the computational determination of the least squares minimization.

9. CHIRAL VS. NON-CHIRAL POTENTIALS

In common with the analysis presented in the previous sections, much of the early work on phase-shift analysis was undertaken long before the advent of QCD, so the NN potentials were at most considered to be derivable from Quantum Field Theory in purely hadronic terms. This implies in particular the One-Pion-Exchange potential, which has survived over the years, and the Two-Pion-Exchange which has been changing depending on the computational scheme since the first attempts in the early 50's (see e.g., Machleidt [14] for a historical review, in particular about the meson exchange picture).

TABLE 9 | Potential integrals in different partial waves.

	DqS-OPE	DS-χTPE	DS-Born	Gauss-OPE	Gauss-χTPE	Gauss-Born	Compilation
$\widetilde{C}_{^1S_0}$	–0.141(1)	–0.135(2)	–0.128(2)	–0.121(5)	–0.113(9)	–0.133(3)	–0.13(1)
$C_{^1S_0}$	4.17(2)	4.12(2)	4.04(1)	4.20(2)	4.16(2)	4.18(1)	4.15(6)
$D^1_{^1S_0}$	–448.8(11)	443.7(5)	–441.5(3)	–447.0(10)	–446.7(2)	–446.3(2)	–445.7(26)
$D^2_{^1S_0}$	–134.6(3)	–133.1(1)	–132.46(4)	–134.1(3)	–134.02(7)	–133.90(7)	–133.7(8)
$\widetilde{C}_{^3S_1}$	–0.064(2)	–0.038(1)	–0.039(1)	–0.070(2)	–0.019(6)	–0.038(4)	–0.045(19)
$C_{^3S_1}$	3.79(1)	3.55(1)	3.52(1)	4.09(2)	3.785(9)	3.724(9)	3.7(2)
$D^1_{^3S_1}$	–510.7(3)	–504.7(4)	–504.1(2)	–516.7(6)	–509.7(1)	–508.2(1)	–509.0(46)
$D^2_{^3S_1}$	–153.2(1)	–151.4(1)	–151.22(6)	–155.0(2)	–152.90(3)	–152.47(3)	–152.7(14)
$C_{^1P_1}$	6.44(2)	6.54(1)	6.464(6)	6.37(2)	6.529(7)	6.488(7)	6.47(6)
$D_{^1P_1}$	–594.9(2)	–592.1(2)	–590.21(6)	–594.5(2)	-597.83(7)	-596.25(7)	-594.3(28)
$C_{^3P_1}$	3.738(2)	3.659(3)	3.633(3)	3.762(6)	3.677(3)	3.599(1)	3.68(6)
$D_{^3P_1}$	–253.29(5)	–249.8(2)	–249.62(7)	–254.23(9)	-251.0(2)	-251.06(2)	-251.5(19)
$C_{^3P_0}$	–4.911(8)	–4.882(5)	–4.897(3)	–4.944(6)	–4.802(8)	–4.883(2)	–4.89(5)
$D_{^3P_0}$	347.0(2)	343.6(2)	344.62(6)	345.8(1)	345.02(3)	346.25(2)	345.4(12)
$C_{^3P_2}$	–0.445(2)	–0.434(3)	–0.426(2)	–0.426(2)	–0.448(1)	–0.427(1)	–0.43(1)
$D_{^3P_2}$	–10.62(7)	–9.7(2)	-9.45(6)	–11.55(4)	–9.939(8)	–9.631(7)	–10.1(8)
$D_{^1D_2}$	–70.92(3)	–70.66(6)	–70.52(3)	–70.58(3)	-7-1.109(7)	–71.074(5)	–70.8(3)
$D_{^3D_2}$	–367.8(2)	–364.39(7)	–364.54(4)	–367.19(8)	–367.10(2)	–366.99(1)	-366.3(15)
$D_{^3D_1}$	205.8(2)	204.25(7)	204.26(4)	204.4(1)	205.17(3)	205.21(3)	204.9(6)
$D_{^3D_3}$	0.55(1)	0.87(6)	0.90(4)	–0.32(9)	0.26(3)	0.51(3)	0.46(45)
C_{ϵ_1}	–8.36(2)	–8.500(4)	–8.492(4)	–8.35(1)	–8.404(4)	–8.399(5)	–8.42(7)
$D^1_{\epsilon_1}$	1012.6(6)	1005.5(1)	1006.23(6)	1010.5(3)	1011.83(5)	1012.71(6)	1009.9(32)
$D^2_{\epsilon_1}$	434.0(3)	430.94(4)	431.24(3)	433.1(1)	433.64(2)	434.02(2)	432.8(14)
D_{ϵ_2}	84.18(4)	83.29(1)	83.398(7)	84.25(3)	83.660(5)	83.818(8)	83.8(4)

Errors quoted for each potential are statistical; errors in the last column are systematic and correspond to the sample standard deviation of the six previous columns. See main text for details on the calculation of systematic errors. Units are: $\widetilde{C}$'s are in 10^4 GeV^{-2}, C's are in 10^4 GeV^{-4}, and D's are in 10^4 GeV^{-6}.

After the appearance of QCD as a fundamental theory of strong interactions there emerged dedicated studies on the underlying quark dynamics in terms of quark cluster models, particularly concerning the origin of the nuclear core (see e.g., [92–94] and references therein). Despite the numerous attempts it is fair to say that these investigations did provide some microscopic and quantitative understanding of the short range components of the interaction but did not offer an alternative to the conventional partial wave analysis. Current QCD potentials determined on the lattice [36–38, 44], are still less precise than phenomenological ones.

In the early 90's Weinberg [95] (see e.g., [96–98] for comprehensive reviews and references therein) proposed an Effective Field Theory (EFT) approach to NN scattering based on chiral symmetry directly inspired by QCD features, where the spontaneous breakdown of chiral symmetry underlies the would-be Goldstone boson nature of the pion. As compared to the phenomenological approaches, the attractive pattern of such an EFT was also the natural hierarchy of n-body forces and the possibility of making an *a priori* estimate of the systematic uncertainties in terms of a power counting to different orders. This happened at about the time when the phenomenological approach harvested its great success when the Nijmegen group obtained for the first time a statistically acceptable $\chi^2/\nu \sim 1$ by fitting and selecting np+pp scattering data. Comprehensive fits to data with chiral interactions have been made using the N2LO chiral potentials [99] to the Nijmegen database [15] for pp [100] and for pp+np [101] and the N3LO chiral potential [102] to the enlarged database [18] for np [103]. The newest generation of chiral potentials have already provided fits to the Granada-2013 database [40, 48, 77, 104–108].

9.1. Statistical Issues

Very recently chiral potentials to sixth order in the chiral expansion have been been claimed by the Bochum group to outperform the non-chiral potentials on the basis of the Granada-2013 database [107]. This was a major achievement of the chiral approach (see also [108] for a momentum space approach of the Idaho-Salamanca group). Another great advantage of the chiral approach is that the number of fitting parameters is substantially smaller than in the phenomenological approach. In no case, however, have the authors taken seriously the available statistical tests to verify *a posteriori* the normality of residuals.

Within the uncertainty quantification context, a critical analysis with an eye on the future developments has been put forward in Ruiz Arriola et al. [109] and Navarro Perez and Ruiz Arriola [43]. It has been suggested that a further order in the expansion, namely N5LO, might quite likely achieve the desired statistical consistency. At the present state, however, there are still some pending, hopefully manageable, issues which need to be resolved before the validation of the chiral approach to NN scattering can be declared without reservations.

9.2. The Chiral Tensorial Structure

For instance, the tensorial structure of the force requires phenomenologically that all allowed NN components should contribute to some extent to the total NN potential. Chiral perturbation theory proposes a hierarchy among the different components so that the chiral W_Q component vanishes to N4LO, unlike all the phenomenological analyses so far [43]. In addition, the number of independent parameters in a scheme where W_Q would be non-vanishing becomes comparable to the phenomenological potentials.

9.3. Peripheral Waves

One of the reasons why the coupling constants discussed in section 6 can be pinned down so accurately [60, 61] is given by the fact that long distant physics is rather well-determined. From that point of view one expects that peripheral waves are rather sensitive to the shape of the potential and hence become independent of the short range components. This also provides a method to validate other analyses and in particular chiral potentials. A very vivid way of presenting the discrepancy is by comparing the phase-shifts in terms of the impact parameter variable [110] (see Equation 74) for every partial wave

$$\xi^{\rm N4LO}(b) = \left. \frac{\delta_l^{\rm N4LO} - {\rm Mean}(\delta_l)}{{\rm Std}(\delta_l)} \right|_{l+1/2=bp}, \qquad (82)$$

which provides a measure of the discrepancy with respect to a set of phase-shifts (see **Figure 2** for a plot of different sets). The conclusion of Simo et al. [110] is quite unequivocal: In the range 2 fm $\leq b \leq$ 5 fm the $\delta^{\rm N4LO}$ differ by more than 3σ when compared to the primary Granada 2013 analysis for F, G, and H waves, and become 1σ compatible with the spread of the 13 high quality potentials.

9.4. Perturbation Theory for Higher Partial Waves

The long distance character of chiral potentials suggests that one may determine the high peripheral partial waves in perturbation theory, as done explicitly in Entem et al. [111]. Actually, the low energy parameters discussed above in section 8.1 probe the longest distance features of a given partial wave. Going to N2LO one sees that, while there is some rough agreement between the perturbative and the full low energy parameters, the detailed comparison including both statistical and systematic errors do not agree. Using the perturbative version of the variable phase approach, a perturbative evaluation [43] in the context of chiral TPE (N2LO in the chiral expansion) was also undertaken and shown *not* to converge to the exact result within uncertainties, even at the largest angular momenta and hence for the most peripheral waves.

9.5. Coarse Graining Chiral Potentials

Chiral potentials can be combined with coarse graining in a statistically consistent way [48, 48, 77, 104]. This allows for a reduction of parameters to about 30 since the separation distance can be made as small as $r_c = 1.8$ fm without spoiling the statistical analysis. This approach assumes the chiral power counting for the potential *above* r_c but not in the coarse grained region so that the all the potential components (including the chirally missing W_Q) are non-vanishing, and taking $f^2 = 0.0075$ has provided natural values for the chiral constants $(c_1, c_3, c_4) =$

$(-0.41 \pm 1.08, -4.66 \pm 0.60, 4.31 \pm 0.17)\text{GeV}^{-1}$ for $T_{\rm LAB} \leq$ 350MeV [48, 77].

In contrast, the canonical (Weinberg) power counting scheme applies to the *full* potential and only to at least N5LO provides all non-vanishing tensorial components ($W_Q = 0$ at N4LO), in which case the number of parameters becomes comparable with the phenomenological approach. As emphasized in Navarro Perez and Ruiz Arriola [43], the end of the chiral road-map in NN scattering based on the power counting will definitely occur when such a scheme becomes reliable enough to select and fit scattering data, without explicit reference to the phenomenological approach.

10. BINDING IN LIGHT NUCLEI: ERROR PROPAGATION

Much of the previous analysis may be used to analyze the impact of NN scattering uncertainties to binding energies. A precursor of this type of calculations was carried out in Adam et al. [21] where estimates on binding uncertainties were carried out using a statistical regularization of phases and a direct solution of the inverse scattering problem.

10.1. On-Shell vs. Off-Shell

NN Scattering data describe only the behavior of nucleons on-shell, i.e., with $E_p = \sqrt{p^2 + M^2}$ in the relativistic case. However, nuclear structure calculations usually need also the corresponding off-shell components so that when going from the NN scattering data to the binding energy calculation some extra information would be needed [35]. This ambiguity can be used in fact to our benefit, since ideally one would determine the off-shellness from the determination of the finite nuclei properties. The successful attempts by Vary et al. are a good demonstration of that [112, 113]

10.2. Computational vs. Physical Precision

Let us review the sources of numerical precision in the solution of the quantum-mechanical problem. In the simplest NN case, where we usually solve numerically the two-body Schrödinger equation, the precision is fixed by the precision in the wave function. In the positive energy situation corresponding to a scattering state we are rather interested in the determination of the scattering phase-shifts.

Within the few-body community there has been a trend to determine the quantum mechanical solution with an increasing pre-defined precision, say, a 1%. This is a pure conventional precision which has been a goal *per se* and, of course, good precision is not disturbing provided the computational cost does not scale up to an unbearable limit where the calculation becomes unfeasible. However, this does not correspond to the *physical* precision where all necessary effects are taken into account and which determines in fact the predictive power of the theory.

10.3. Monte Carlo Method

The normality property of the residuals has been exploited to extract the effective interaction parameters and corresponding counter-terms [54] and to replicate via Monte Carlo bootstrap simulation as a mean to gather more robust information on the uncertainty characteristics of fitting parameters [83]. We stress that the verification of normality, Equation (54), is essential for a meaningful propagation of the statistical error, since the uncertainty inherited from the fitted scattering data $\Delta O_i^{\rm exp}$ corresponds to a genuine statistical fluctuation. This allows to determine the 1σ error of the parameters $\mathbf{p} = \mathbf{p}_0 \pm \Delta\mathbf{p}^{\rm stat}$ and hence the error in the potential

$$V_{NN} = V_{NN}(\mathbf{p}_0) \pm \Delta V_{NN}^{\rm stat} \tag{83}$$

which generates in turn the error in the NN phase-shifs $\delta = \delta(\mathbf{p_0}) \pm \Delta\delta^{\rm stat}$ and mixing angles. Once the NN-potential is determined the few body problem can be solved for the binding energy,

$$\left[\sum_i T_i + \sum_{i<j} V_{NN}(ij)\right]\Psi = E_A\Psi \tag{84}$$

where

$$E_A = E_A(\mathbf{p}_0) \pm \Delta E_A^{\rm stat}\,. \tag{85}$$

Direct methods to determine $\Delta\mathbf{p}^{\rm stat}$, $\Delta V_{NN}^{\rm stat}$ and $\Delta E_A^{\rm stat}$ proceed either by the standard error matrix or Monte Carlo methods (see e.g., [68]). In Navarro Pérez et al. [83] we have shown that the latter method is more convenient for large number of fitting parameters (typically $N_P = 40 - 60$), and consists of generating a sufficiently large sample drawn from a multivariate normal probability distribution

$$P(p_1, p_2, \ldots, p_P) = \frac{1}{\sqrt{(2\pi)^{N_P}\det\mathcal{E}}} e^{-\frac{1}{2}(\mathbf{p}-\mathbf{p}_0)^T\mathcal{E}^{-1}(\mathbf{p}-\mathbf{p}_0)}, \tag{86}$$

where $\mathcal{E}_{ij} = (\partial^2\chi/\partial p_i\partial p_j)^{-1}$ is the error matrix. We generate M samples $\mathbf{p}_\alpha \in P$ with $\alpha = 1, \ldots, M$, and compute $V_{NN}(\mathbf{p}_\alpha)$ from which the corresponding scattering phase shifts $\delta(\mathbf{p}_\alpha)$ and binding energies $E_A(\mathbf{p}_\alpha)$ can be determined. Of course, one drawback of the MonteCarlo propagation method is that the object function, in this case the energy, needs to be evaluated a sufficiently large number of times which may be unduly time consuming. An analysis of statistical errors at the phase shift level shows that $M = 25$ may be sufficient to reproduce consistently the covariance matrix uncertainties from the MonteCarlo method.

10.4. The Deuteron

The deuteron is the simplest bound nuclear np system for which the theory has long been developed [114]. Its quantum numbers $J^P = 1^+$ correspond to the coupled ${}^3S_1 - {}^3D_1$ channel with reduced wave functions $u(r)$ and $w(r)$ respectively, so that we solve the bound state problem with $E_d = -B_d = -\gamma^2/2\mu_{np}$, i.e., with $p = i\gamma$. At long distances

$$u(r) \to A_S e^{-\gamma r}, \qquad w(r) \to \eta A_S e^{-\gamma r}\left[1 + \frac{3}{\gamma r} + \frac{3}{(\gamma r)^2}\right] \tag{87}$$

For normalized states we list in **Table 10** the asymptotic D/S ratio η, asymptotic S-wave amplitude A_S, mean squared matter radius r_m, quadrupole moment Q_D, D-wave probability P_D and inverse matter radius $\langle r^{-1} \rangle$ for some high quality potentials compared with two Granada potentials, DS-OPE [45], DS-TPE [77]. The PWA analysis indeed uses its binding energy as a fitting parameter, so that the quoted uncertainties are purely statistical. Unlike r_m, Q_D, or P_D which require (small) meson exchange currents corrections before being compared to experimental data, A_S and η are purely hadronic. As we see, both the DS-OPE [77] DS-TPE [77] provide *smaller* uncertainties than the experimental/recommended values for A_S and η. To our knowledge, this is an unprecedented situation in Nuclear Physics. Similar trends are also observed for the corresponding deuteron charge, magnetic and quadrupole form factors (see e.g., [121] for a review) where DS-OPE [45] and DS-TPE [77, 122] generate tiny uncertainties and offer an opportunity to discriminate meson exchange currents contributions.

10.5. Binding Energies for A = 3,4 Systems

The primary Granada DS-OPE potential which was used to fit and select np+pp scattering data uses Dirac delta-shells which are too singular in configuration space or have too long momentum tails, for instance in the deuteron [26], to be handled in few body calculations. Actually, this was the reason to design smooth SOG (Sum of Gaussian) potentials [53, 75] referenced in section 7.

In Navarro Perez et al. [24] the triton binding energy was evaluated for the SOG-OPE Granada potential using the hyperspherical harmonics method with $M \sim 200$ MonteCarlo replicas, and statistical distributions where also obtained yielding $\Delta E_t = 12$ KeV. One motivation for such a calculation was to determine if the computational accuracy was unnecessarily better than the statistical accuracy inherited from the NN scattering data. Our points are illustrated in **Table 11** from Navarro Perez et al. [24] where the numerical convergence regarding the number of partial waves is displayed. The error estimate clearly marks where the accuracy of the numerical calculation is larger than the physical accuracy.

The statistical uncertainty of experimental NN scattering data have also been propagated into the binding energy of ^{3}H and ^{4}He using the no-core full configuration method in a sufficiently large harmonic oscillator basis. The error analysis [26] yields $\Delta B_t = 15$ KeV and $\Delta B_\alpha = 55$ KeV.

Similar patterns occur when solving the Faddeev equations for ^{3}H and the Yakubovsky equations for ^{4}He respectively [25]. We check that in practice about $M = 30$ samples prove enough for a reliable error estimate within the MonteCarlo method, giving $\Delta B_t = 12$ KeV and $\Delta B_\alpha = 50$ KeV whereas, again, the computational accuracy is better, $\Delta B_t^{\rm num} = 1$ KeV and $\Delta B_\alpha^{\rm num} = 20$ KeV.

Results for the 3N and 4N binding energies for various NN potentials using the Faddeev equations for ^{3}H and the Yakubovsky equations for ^{4}He are listed in **Table 12** where we see a systematic underbinding with respect to the experimental values. A popular interpretation of this disagreement suggests that the influence of three- and four-body forces has been neglected. However, the contribution of three body forces depends on the definition of two body forces as we will discuss next.

10.6. The Tjon Line

Much of the error analysis which can and has been carried out in Nuclear Physics is probably best exemplified by the so called Tjon

TABLE 11 | Triton binding energy convergence for the hyper-spherical harmonics method [24] in the number of channels, N_c, classified according to the orbital angular momentum of the pair $L_{\rm Pair}$ and the spectator $l_{\rm spectator}$ in the triton as the number of total accumulated channels, $N_{\rm Total}$, is increased.

N_c	$L_{\rm Pair}$ $l_{\rm Spectator}$	$N_{\rm Total}$	Energy (MeV)
3	Ss	3	Unbound
+2	Sd+Ds	5	–7.0117
+10	Pp	15	–6.4377
+8	Dd	23	–7.4109
+4	Pf+Fp	27	–7.4956
+10	Ff	37	–7.5654
+2	Dg+Gd	39	–7.6178
+8	Gg	47	–7.6502
+4	Fh+Hf	51	–7.6508
+10	Hh	61	–7.6510

The potential used was Monte Carlo generated. A horizontal line is drawn when the change in E_t is smaller than the statistical uncertainty $\Delta B_t = 15(1)$ keV.

TABLE 10 | Deuteron static properties compared with empirical/recommended values [115–120] and high-quality potentials calculations, DS-OPE [45], DS-TPE [77], Nijm I [16], Nijm II [16], Reid93 [16], AV18 [17], CD-Bonn [18].

	Emp./Rec.	DS-OPE	DS-TPE	Nijm I	Nijm II	Reid93	AV18	CD-Bonn
E_d(MeV)	2.224575(9)	Input	Input	Input	Input	Input	Input	Input
η	0.0256(5)	0.02493(8)	0.02473(4)	0.02534	0.02521	0.02514	0.0250	0.0256
A_S(fm$^{1/2}$)	0.8845(8)	0.8829(4)	0.8854(2)	0.8841	0.8845	0.8853	0.8850	0.8846
r_m(fm)	1.971(6)	1.9645(9)	1.9689(4)	1.9666	1.9675	1.9686	1.967	1.966
Q_D(fm^2)	0.2859(3)	0.2679(9)	0.2658(5)	0.2719	0.2707	0.2703	0.270	0.270
P_D	5.67(4)	5.62(5)	5.30(3)	5.664	5.635	5.699	5.76	4.85
$\langle r^{-1} \rangle$(fm^{-1})		0.4540(5)	0.4542(2)		0.4502	0.4515		

We list binding energy E_d, asymptotic D/S ratio η, asymptotic S-wave amplitude A_S, mean squared matter radius r_m, quadrupole moment Q_D, D-wave probability P_D, and inverse matter radius $\langle r^{-1} \rangle$.

TABLE 12 | 3N and 4N binding energies for various NN potentials using the Faddeev equations for ^{3}H and the Yakubovsky equations for ^{4}He respectively [25, 123].

Potential	Exp.	SOG-OPE	CD Bonn	AV18	Nijm I	Nijm II	Nijm93
^{3}H [MeV]	−8.4820(1)	−7.660(12)	−8.012	−7.623	−7.736	−7.654	−7.668
^{4}He [MeV]	−28.2957(1)	−24.760(47)	−26.26	−24.28	−24.98	−24.56	−24.53

Errors in SOG-OPE are statistical.

line [34], a linear but empirical correlation between the triton and α-particle binding energies of the form

$$B_\alpha = aB_t + c \tag{88}$$

where a, c depend on a family of NN potentials which have the *same* NN scattering phase shifts and deuteron properties. Thus, the slope may be schematically be written as $a = (\partial B_\alpha/\partial B_t)|_{B_d}$. This empirical feature [124, 125] comparing between phase-equivalent potentials has been corroborated by many calculations ever since [123, 126, 127]. It is remarkable that such a simple property has no obvious explanation. One clue would be the fact that the deuteron binding energy, $B_d = 2.2$ MeV, is small compared to the triton and alpha bindings [128]. For small B_d the alpha binding energy then would scale as $B_\alpha = aB_t + bB_d + \mathcal{O}(B_d^2)$. The points along this line in the plane (B_t, B_α) correspond to potentials with the same phase-shifts, verifying $\Delta B_\alpha = a\Delta B_t$ The points along a perpendicular line, $\Delta B_\alpha = -1/a\Delta B_t$ should correspond to potentials with very different phase-shifts. In particular the difference may be generated by a unitary transformation of the NN potential, $V_2 \to UV_2U^\dagger$, so that the bindings depend on U but the coefficients a and b do not depend on U [123]. On the other hand, a unitary transformation of the *two-body* potential implies a change in multi-nucleon forces, V_3, V_4, etc. and, one may actually fit E_t with a suitable V_3 and E_α with a suitable V_4 yielding for $V_4 = 0$ in the so-called on-shell limit the formula $B_\alpha = 4B_t - 3B_d$ which works well [129, 130].

Phase equivalent interactions produce a Tjon slope which is typically about $\Delta B_\alpha/\Delta B_t \sim 5 - 6$ both in the Faddeev-Yakubovsky [126] and in the no-core shell model [131]. For the Faddeev-Yakubovsky solutions of ^{3}H-^{4}He the results from five high quality potentials, i.e., with $\chi^2/\nu \sim 1$ at their time and the Granada SOG-OPE, in **Table 12** give $B_\alpha = 4.73B_t - 5.26B_d$. For a sample of SOG-OPE potentials the statistical bootstrap analysis with $M = 30$ gives $B_\alpha = 4.8(1)B_t - 5.4(3)B_d$, where the central values reflect the actual scattering data and the uncertainties reflect the truly phase-inequivalent fluctuations. The extrapolation predicts the experimental binding of the alpha particle within uncertainties [25], since

$$\Delta B_\alpha^2|_{\rm stat} = (\Delta a)^2 B_t^2 + (\Delta b)^2 B_d^2 \tag{89}$$

so that $\Delta B_\alpha|_{\rm stat} \sim 1$MeV. Interestingly, this suggests a marginal effect of four body forces, for which independent estimates using approximate wave functions [132] give similar numbers, $B_\alpha|_{4N} \sim -100$ KeV (see also Epelbaum [133] for a chiral scheme where this is argued to overestimate the result). Thus, we see that since $B_\alpha|_{4N} \sim \Delta B_\alpha^{\rm stat}$ the four-body force might be unobservable. While this is good news from the theoretical point of view, more detailed calculations might be needed to confirm this feature. Finally, let us also mention that along these lines, theoretical uncertainties of the elastic nucleon-deuteron scattering observables have been undertaken [27].

11. EFFECTIVE NUCLEAR INTERACTIONS

11.1. Moshinsky-Skyrme Parameters

Power expansions in momentum space of effective interactions were introduced by Moshinsky [134] and Skyrme [135] to provide significant simplifications to the nuclear many body problem in comparison with the *ab initio* approach, in which it is customary to employ phenomenological interactions fitted to NN scattering data to solve the nuclear many body problem. As a consequence of such simplifications effective interactions, also called Skyrme forces, have been extensively used in mean field calculations [136–139]. Within this framework the effective force is deduced from the elementary NN interaction and encodes the relevant physical properties in terms of a small set of parameters. However, there is not a unique determination of the Skyrme force and different fitting strategies result in different effective potentials (see e.g., [140] and [141]). This diversity of effective interactions within the various available schemes signals a source of statistical and systematic uncertainties that remain to be quantified. Fortunately the parameters determining a Skyrme force can be extracted from phenomenological interactions [88, 142] and uncertainties can be propagated accordingly [54]. At the two body level the Moshinsky-Skyrme potential in momentum representation reads

$$\begin{aligned} V_\Lambda(\mathbf{p}', \mathbf{p}) &= \int d^3x e^{-i\mathbf{x}\cdot(\mathbf{p}'-\mathbf{p})} \hat{V}(\mathbf{x}) \\ &= t_0(1 + x_0P_\sigma) + \frac{t_1}{2}(1 + x_1P_\sigma)(\mathbf{p}'^2 + \mathbf{p}^2) \\ &+ t_2(1 + x_2P_\sigma)\mathbf{p}' \cdot \mathbf{p} + 2iW_0\mathbf{S} \cdot (\mathbf{p}' \times \mathbf{p}) \\ &+ \frac{t_T}{2}\left[\sigma_1 \cdot \mathbf{p}\,\sigma_2 \cdot \mathbf{p} + \sigma_1 \cdot \mathbf{p}'\,\sigma_2 \cdot \mathbf{p}'\right. \\ &\left. -\frac{1}{3}\sigma_1 \cdot \sigma_2(\mathbf{p}'^2 + \mathbf{p}^2)\right] \\ &+ \frac{t_U}{2}\left[\sigma_1 \cdot \mathbf{p}\,\sigma_2 \cdot \mathbf{p}' + \sigma_1 \cdot \mathbf{p}'\,\sigma_2 \cdot \mathbf{p} - \frac{2}{3}\sigma_1 \cdot \sigma_2\mathbf{p}' \cdot \mathbf{p}\right] \\ &+ \mathcal{O}(p^4) \end{aligned} \tag{90}$$

where $P_\sigma = (1 + \sigma_1 \cdot \sigma_2)/2$ is the spin exchange operator with $P_\sigma = -1$ for spin singlet $S = 0$ and $P_\sigma = 1$ for spin triplet $S = 1$ states. These parameters correspond to radial moments of volume integrals of the potentials $\int_0^\infty d^3x r^n V_i(r)$ which are increasingly insensitive to short distances.

As mentioned above different nuclear data can be used to constrain the Skyrme potential. The usual approach is to fit parameters of Equation (90) to doubly closed shell nuclei and nuclear matter saturation properties [136–139]. In Ruiz Arriola [142] the parameters were determined from just NN threshold properties such as scattering lengths, effective ranges

and volumes without explicitly taking into account the finite range of the NN interaction; while in Navarro Perez et al. [88] the parameters were computed directly from a local interaction in coordinate space that reproduces NN elastic scattering data. In Navarro Pérez et al. [54] the latter approach was used to propagate *statistical* uncertainties into the Skyrme parameters. The quantification of the *systematic* uncertainties, which arise from the different representations of the NN interaction was discussed in Navarro Perez et al. [87]. The results, summarized in **Table 13** clearly show, again, the dominance of systematic vs statistical errors.

11.2. Error Estimates for Heavy Nuclei and Nuclear Matter

Within the Skyrme effective interactions approach one can find a simple estimate of systematic errors due to the two body interaction uncertainty using (for a review see [139])

$$\frac{\Delta B}{A} = \frac{3}{8A}\Delta t_0 \int d^3x\, \rho(x)^2, \tag{91}$$

For nuclear matter at saturation, $\rho_0 = 0.17\text{fm}^{-3}$, our $\Delta t_0 = 75\text{MeV fm}^3$ implies

$$\frac{\Delta B}{A} = \frac{3}{8}\Delta t_0 \rho_0 = 2.4\text{MeV}. \tag{92}$$

We may implement finite size effects in light-heavy nuclei by using a Fermi-type shape for the matter density

$$\rho(r) = C/(1 + e^{(r-R)/a}) \tag{93}$$

with $R = r_0 A^{\frac{1}{3}}$, $r_0 = 1.1\,\text{fm}$ and $a = 0.7\,\text{fm}$, Normalizing to the total number of particles $A = \int d^3x\rho(x)$ we get values in the range

$$\Delta B_A/A = 0.4 - 1.6\text{MeV}, \tag{94}$$

depending on the value of A for $4 \leq A \leq 208$.

12. COARSE GRAINED POTENTIAL RESULTS

Besides the aspect of uncertainty quantification which is the focus of the present work, we believe that the very idea of coarse graining proves useful in nuclear physics. This requires that special methods have to be developed for delta–shells interaction, which in our view are the most flexible ones which allow for selecting and fitting the largest NN database to date, but cannot be plugged directly in conventional computing codes dealing with nuclear structure and reactions, and hence smooth potentials (such as the SOG-Granada type potentials) need to be defined *after* the data selection process. This is similar to what happened with the energy dependence needed by the Nijmegen group which also led to subsequent high quality interactions. We discuss here some simple examples where delta-shells may be used *directly*.

12.1. Repulsive vs. Structural Core

Besides the well-accepted OPE mechanism for long distances and the mid-range attraction which is needed for nuclear binding, one of the traditional and well-accepted properties of the nuclear potential is the existence of a nuclear strongly repulsive core at about 0.5 fm. While this feature guarantees the stability of nuclei and nuclear matter against collapse it also complicates the solution of the many body problem, since the relative NN wave function must vanish below the core, therefore introducing a very strong short range correlation. At a practical level the existence of the core implies a vanishing of the wave function at about the core location, but something else is needed to determine the wave function below the core radius. The question is whether the repulsive core is indispensable from the analysis of collision experiments. However, in order to resolve the core in NN elastic scattering one needs a wavelength which corresponds to energies where there is a substantial in-elasticity and hence a complex optical potential is needed in order to deal with the absorption due to inelastic processes such as $NN \to NN\pi$. This point has been analyzed in Fernandez-Soler and Ruiz Arriola [46] and it has been

TABLE 13 | Moshinsky-Skyrme parameters for the renormalization scale $\Lambda = 400$ MeV.

	DS-OPE	DS-χTPE	DS-Born	Gauss-OPE	Gauss-χTPE	Gauss-Born	Compilation
t_0	–626.8(64)	–529.6(53)	–509.0(55)	–584.4(157)	–406.1(289)	–521.8(152)	-529.6(751)
x_0	–0.38(2)	–0.56(1)	–0.54(1)	–0.26(2)	–0.71(8)	–0.55(4)	–0.50(16)
t_1	948.1(30)	913.6(22)	900.1(17)	987.4(29)	945.5(18)	941.3(16)	939.3(304)
x_1	–0.048(3)	–0.074(3)	–0.068(3)	–0.013(3)	–0.047(3)	–0.058(2)	–0.051(22)
t_2	2462.6(56)	2490.0(39)	2462.1(25)	2441.3(56)	2490.1(24)	2466.8(26)	2468.8(187)
x_2	–0.8686(6)	–0.8750(8)	–0.8753(6)	–0.8630(8)	–0.8729(6)	–0.8785(3)	–0.872(6)
W_0	107.7(4)	100.8(3)	96.2(3)	105.0(5)	109.3(7)	94.3(2)	102.2(61)
t_U	1278.6(12)	1260.3(5)	1257.0(4)	1285.6(12)	1254.9(9)	1249.3(3)	1264.3(144)
t_T	–4220.9(87)	–4292.8(23)	–4289.0(21)	–4385.6(99)	–4271.8(51)	–4319.5(58)	–4296.6(545)

Errors quoted for each potential are statistical; errors in the last column are systematic and correspond to the sample standard deviation of the six previous columns. See main text for details on the calculation of systematic errors. Units are: t_0 in MeVfm^3, t_1, t_2, W_0, t_U, t_T in MeVfm^5, and x_0, x_1, x_2 are dimensionless.

found that there exist two solutions, one corresponding to the usual repulsive core and the other one related to the so-called structural core, reminiscent of the composite character of the nucleon.

12.2. Coarse Graining Short Range Correlations

The Bethe-Goldstone equation [143, 144] has been a way to describe short range correlations between nucleons inside the nucleus. In the nuclear medium the interaction produces no scattering due to the Pauli principle. Instead the relative wave function of a pair is modified in presence of the two-body interaction, generating high-momentum components above the Fermi momentum, $p > p_F$. Using the delta-shell potential allows to simplify the problem of computing these high momentum components arising in an interacting nucleon pair in nuclear matter. This coarse graining of the Bethe-Goldstone equation has been explored in Ruiz Simo et al. [145, 146] for back-to-back nucleons, with total center of mass momentum equal to zero. The formalism still has to be extended to other values of the center of mass.

12.3. Error Analysis of Nuclear Matrix Elements

The expected errors of harmonic oscillator nuclear matrix elements coming from the uncertainty on the NN interaction have been estimated in Amaro et al. [147] for the coarse grained (GR) interaction fitted to NN scattering data, with several prescriptions for the long-part of the interaction, including one pion exchange and chiral two-pion exchange interactions.

12.4. Shell Model Estimates

In a previous calculation [51], we showed how our approach is competitive not only as a way of determining the phase shifts but also compared to more sophisticated approaches to Nuclear Structure [148]. We computed the ground state energy of several closed-shell nuclei by using oscillator wave functions. In the case of ^{4}He, ^{16}O, and ^{40}Ca nuclei, our calculation reproduces the experiment at the $20-30\%$-level provided the phase-shifts are fitted up to energy $E \leq 100$MeV [51]. This is a tolerable accuracy as we just intend to make a first estimate on the systematic uncertainties and then compute the change in the binding energy. For the $A = 3, 4$ nuclei we use the simple formulas,

$$\Delta B(^3\mathrm{H}) = \langle \Delta V_2 \rangle_{^3\mathrm{H}} = 3\langle 1s| \frac{1}{2} \left(\Delta V_{^1S_0} + \Delta V_{^3S_1} \right) |1s\rangle, \quad (95)$$

$$\Delta B(^4\mathrm{He}) = \langle \Delta V_2 \rangle_{^4\mathrm{He}} = 6\langle 1s| \frac{1}{2} \left(\Delta V_{^1S_0} + \Delta V_{^3S_1} \right) |1s\rangle, \quad (96)$$

where $|1s\rangle$ is the Harmonic oscillator relative wave function with the corresponding oscillator parameter b fixed to reproduce the physical charge radius. The factors in front of the matrix elements are Talmi-Moshinsky coefficients corresponding in this particular case to the number of pairs interacting through a relative s-wave. Errors in the potential ΔV are computed by adding individual contributions $(\Delta\lambda_n)^{JS}_{l,l'}$ in quadrature. By propagating the potential errors to Equation (95) we find

$$\frac{\Delta B(3)}{3} = 0.07 - 0.085\mathrm{MeV} \quad (97)$$

depending on the fitting cut-off LAB energy, 100–350 MeV respectively, overestimating the Faddeev estimates given above. For the $\alpha-$particle Equation (96) yields

$$\frac{\Delta B(4)}{4} = 0.10 - 0.13\mathrm{MeV}. \quad (98)$$

More generally, for heavier double-closed shell nuclei one has along the lines of Navarro Perez et al. [51]

$$\Delta B(A) = \sum_{nlSJ} g_{nlJS} \langle nl|\Delta V^{JST}|nl\rangle \quad (99)$$

where g_{nlJS} depends on the Talmi-Moshinsky brackets. For ^{16}O and ^{40}Ca, we find

$$\frac{\Delta B(^{16}\mathrm{O})}{16} = 0.26\,\mathrm{MeV} \qquad \frac{\Delta B(^{40}\mathrm{Ca})}{40} = 0.32\mathrm{MeV}. \quad (100)$$

These systematic estimates using shell model are of the same order to the ones obtained above in the Skyrme interaction.

13. OUTLOOK

Despite the many years elapsed since the first NN partial wave analysis in 1957 and the huge theoretical and experimental efforts carried out, the nuclear force is poorly known still where it is most needed, namely in the mid-range regime which is relevant for *ab initio* calculation of nuclear binding energies. This is the explanation behind the relatively large uncertainties found in large scale calculations. During many years there has been a conformist attitude regarding these uncertainties, and in most papers a purely computational approach has prevailed, validating theoretical frameworks just on their numerical performance. Only in recent years the issue of uncertainties has been taken seriously, as it is actually the key to establish the predictive power of the theory. Clearly, the level of ambiguity we are dealing with in the evaluation of nuclear uncertainties of all sorts, statistical, systematic, and computational requires a rigorous treatment. In this work we have reviewed this topic from the perspective of the impact of the Granada NN database on the determination of the NN force and its consequences on nuclear binding.

The main theoretical obstacle has to do with the great difficulty in providing a unique definition of the nuclear potential just from data. Quantum field theory at the hadronic level implies the existence of a long range interaction dominated by pion exchanges as the lightest particles and reduces the ambiguity. Lattice calculations of potentials may identify them with static energies assuming heavy quark-composite sources but their accuracy is at present not satisfactory. Chiral perturbation theory provides in addition several schemes based on a power

counting which, while not fully satisfactory, may be and have been implemented in the NN sector and extended to multi-nucleon forces. The consistency among chiral multi-nucleon forces is theoretically very appealing and the use of potentials is possibly the only practical path toward a satisfactory solution of the nuclear many body problem. It should be stressed that the EFT point of view is the most suitable one since in principle one gets rid of the model dependence with *a priori* uncertainty estimates. However, a more detailed analysis reveals that there are issues regarding the necessary regularization of the theory, which effectively model the mid-range regime of the NN interaction. Moreover, the indispensability of the chiral scheme for NN scattering data remains to be proven, not to speak about its suitability for fitting and selecting a NN database itself. At a phenomenological level at the present stage the determination of the NN interaction below 1.8 fm (up to a phase equivalent unitary transformation) remains so far connected to a combination of an abundance of data in a variety of kinematics and observables with the corresponding experimental errors.

In our view, this unfortunate situation on the side of the hadronic theory will likely not necessarily improve neither with more and better experimental measurements nor with larger computational facilities, but with a better understanding on the essence of hadronic interactions and their range of applicability.

AUTHOR CONTRIBUTIONS

All authors listed have made a substantial, direct and intellectual contribution to the work, and approved it for publication.

FUNDING

This work was supported by the Spanish MINECO and European FEDER funds (grant FIS2017-85053-C2-1-P) and Junta de Andalucía (grant FQM-225).

ACKNOWLEDGMENTS

We thank Ignacio Ruiz Simó, James Vary, Pieter Maris, Eduardo Garrido, Andreas Nogga, Rocco Schiavilla, Maria Piarulli, Pedro Fernández Soler, Jacobo Ruiz de Elvira, Varese Salvador Timoteo, and Sergio Szpigel for collaboration on different issues discussed in this paper.

REFERENCES

1. Yukawa H. On the interaction of elementary particles. *Proc Phys Math Soc Jpn.* (1935) **17**:48–57.
2. Bethe HA. The meson theory of nuclear forces I. General theory. *Phys Rev.* (1940) **57**:260–72. doi: 10.1103/PhysRev.57.260
3. Bethe H. The meson theory of nuclear forces. Part 2. Theory of the deuteron. *Phys Rev.* (1940) **57**:390–413. doi: 10.1103/PhysRev.57.390
4. Stapp H, Ypsilantis T, Metropolis N. Phase shift analysis of 310-MeV proton proton scattering experiments. *Phys Rev.* (1957) **105**:302–10. doi: 10.1103/PhysRev.105.302
5. Arndt R, Macgregor M. Chi-squared minimization techniques. *Methods Comput Phys.* (1966) **6**:253.
6. Perring J. Nucleon-nucleon phase shifts at 142 mev. *Nucl Phys.* (1963) **42**:306–12.
7. Arndt RA, MacGregor MH. Determination of the nucleon-nucleon elastic-scattering matrix. iv. comparison of energy-dependent and energy-independent phase-shift analyses. *Phys Rev.* (1966) **141**:873.
8. MacGregor MH, Arndt RA, Wright RM. Determination of the nucleon-nucleon scattering matrix. VII. (p, p) analysis from 0 to 400 MeV. *Phys Rev.* (1968) **169**:1128–48. doi: 10.1103/PhysRev.169.1128
9. Arndt R, Roper L. The use of partial-wave representations in the planning of scattering measurements. application to 330 mev n p scattering. *Nucl Phys.* (1972) **B50**:285–300. doi: 10.1016/S0550-3213(72)80019-1
10. Mac Gregor MH, Moravcsik MJ, Stapp HP. Nucleon-nucleon scattering experiments and their phenomenological analysis. *Annu Rev Nucl Part Sci.* (1960) **10**:291–352. doi: 10.1146/annurev.ns.10.120160.001451
11. Breit G. Aspects of nucleon-nucleon scattering theory. *Rev Mod Phys.* (1962) **34**:766–812. doi: 10.1103/RevModPhys.34.766
12. Signell P. The nuclear potential. In: Baranger M, Vogt E, editors. *Advances in Nuclear Physics*. New York, NY: Springer (1969). p. 223–94.
13. de Swart JJ, Nagels MM. The nucleon-nucleon interaction. *Fortsch Phys.* (1978) **26**:215. doi: 10.1002/prop.19780260402
14. Machleidt R. The Meson theory of nuclear forces and nuclear structure. *Adv Nucl Phys.* (1989) **19**:189–376.
15. Stoks V, Kompl R, Rentmeester M, de Swart J. Partial wave analaysis of all nucleon-nucleon scattering data below 350-MeV. *Phys Rev.* (1993) **C48**:792–815. doi: 10.1103/PhysRevC.48.792
16. Stoks V, Klomp R, Terheggen C, de Swart J. Construction of high quality N N potential models. *Phys Rev.* (1994) **C49**:2950–62. doi: 10.1103/PhysRevC.49.2950
17. Wiringa RB, Stoks V, Schiavilla R. An Accurate nucleon-nucleon potential with charge independence breaking. *Phys Rev.* (1995) **C51**:38–51. doi: 10.1103/PhysRevC.51.38
18. Machleidt R. The High precision, charge dependent Bonn nucleon-nucleon potential (CD-Bonn). *Phys Rev.* (2001) **C63**:024001. doi: 10.1103/PhysRevC.63.024001
19. Gross F, Stadler A. Covariant spectator theory of np scattering: Phase shifts obtained from precision fits to data below 350-MeV. *Phys Rev.* (2008) **C78**:014005. doi: 10.1103/PhysRevC.78.014005
20. Amghar A, Desplanques B. Are all models of the N N interaction independent of each other? *Nucl Phys.* (1995) **A585**:657–92. doi: 10.1016/0375-9474(94)00781-H
21. Adam RM, Fiedeldey H, Sofianos SA, Leeb H. Error propagation from nucleon-nucleon data to three- and four-nucleon binding energies. *Nucl Phys.* (1993) **A559**:157–72. doi: 10.1016/0375-9474(93)90184-Y
22. Navarro Perez R, Amaro JE, Ruiz Arriola E. Error estimates on nuclear binding energies from nucleon-nucleon uncertainties. *arXiv [Preprint]* arXiv:1202.6624 (2012).
23. Navarro Perez R, Amaro JE, Ruiz Arriola E. Nuclear binding energies and NN uncertainties. In: *Sixth International Conference on Quarks and Nuclear Physics* (2012). p. 145. doi: 10.22323/1.157.0145
24. Navarro Perez R, Garrido E, Amaro JE, Ruiz Arriola E. Triton binding energy with realistic statistical uncertainties. *Phys Rev.* (2014) **C90**:047001. doi: 10.1103/PhysRevC.90.047001
25. Navarro Perez R, Nogga A, Amaro JE, Ruiz Arriola E. Binding in light nuclei: statistical NN uncertainties vs Computational accuracy. *J Phys Conf Ser.* (2016) **742**:012001. doi: 10.1088/1742-6596/742/1/012001
26. Navarro Pérez R, Amaro JE, Ruiz Arriola E, Maris P, Vary JP. Statistical error propagation in *ab initio* no-core full configuration calculations of light nuclei. *Phys Rev.* (2015) **C92**:064003. doi: 10.1103/PhysRevC.92.064003

27. Skibinski R, Volkotrub Yu, Golak J, Topolnicki K, Witala H. Theoretical uncertainties of the elastic nucleon-deuteron scattering observables. *Phys Rev.* (2018) **C98**:014001. doi: 10.1103/PhysRevC.98.014001
28. Dobaczewski J, Nazarewicz W, Reinhard PG. Error estimates of theoretical models: a guide. *J Phys.* (2014) **G41**:074001. doi: 10.1088/0954-3899/41/7/074001
29. Toivanen J, Dobaczewski J, Kortelainen M, Mizuyama K. Error analysis of nuclear mass fits. *Phys Rev.* (2008) **C78**:034306. doi: 10.1103/PhysRevC.78.034306
30. Landau RH. *Quantum Mechanics II: A Second Course in Quantum Theory*. New York, NY: John Wiley & Sons (2008).
31. Chadan K, Sabatier PC. *Inverse Problems in Quantum Scattering Theory*. Springer Science & Business Media (2012).
32. Newton RG. *Inverse Schrödinger Scattering in Three Dimensions*. New York, NY: Springer Science & Business Media (2012).
33. Coester F, Cohen S, Day B, Vincent CM. Variation in nuclear-matter binding energies with phase-shift-equivalent two-body potentials. *Phys Rev.* (1970) **C1**:769–76. doi: 10.1103/PhysRevC.1.769
34. Tjon JA. Bound states of 4 He with local interactions. *Phys Lett.* (1975) **56B**:217–20. doi: 10.1016/0370-2693(75)90378-0
35. Srivastava M, Sprung DW. Off-shell behavior of the nucleon-nucleon interaction. In: *Advances in Nuclear Physics*. Springer (1975). p. 121–218.
36. Aoki S, Hatsuda T, Ishii N. Theoretical foundation of the nuclear force in QCD and its applications to central and tensor forces in quenched lattice QCD simulations. *Prog Theor Phys.* (2010) **123**:89–128. doi: 10.1143/PTP.123.89
37. Aoki S. Hadron interactions in lattice QCD. *Prog Part Nucl Phys.* (2011) **66**:687–726. doi: 10.1016/j.ppnp.2011.07.001
38. Aoki S. Nucleon-nucleon interactions via Lattice QCD: methodology. *Eur Phys J.* (2013) **A49**:81. doi: 10.1140/epja/i2013-13081-0
39. Okubo S, Marshak RE. Velocity dependence of the two-nucleon interaction. *Ann Phys.* (1958) **4**:166–79.
40. Piarulli M, Girlanda L, Schiavilla R, Navarro Pérez R, Amaro JE, Ruiz Arriola E. Minimally nonlocal nucleon-nucleon potentials with chiral two-pion exchange including Δ resonances. *Phys Rev.* (2015) **C91**:024003. doi: 10.1103/PhysRevC.91.024003
41. Amghar A, Desplanques B. More about the comparison of local and nonlocal NN interaction models. *Nucl Phys.* (2003) **A714**:502–34. doi: 10.1016/S0375-9474(02)01375-1
42. Navarro Pérez R, Amaro JE, Ruiz Arriola E. Coarse-grained potential analysis of neutron-proton and proton-proton scattering below the pion production threshold. *Phys Rev.* (2013) **C88**:064002. doi: 10.1103/PhysRevC.88.064002
43. Navarro Pérez R, Ruiz Arriola E. Uncertainty quantification and falsification of Chiral Nuclear Potentials (2019).
44. Walker-Loud A. Nuclear physics review. In: *31st International Symposium on Lattice Field Theory - LATTICE 2013*. (2014). p. 013. doi: 10.22323/1.187.0013
45. Navarro Pérez R, Amaro JE, Ruiz Arriola E. Partial wave analysis of nucleon-nucleon scattering below pion production threshold. *Phys Rev.* (2013) **C88**:024002. doi: 10.1103/PhysRevC.88.024002
46. Fernandez-Soler P, Ruiz Arriola E. Coarse graining of NN inelastic interactions up to 3 GeV: repulsive versus structural core. *Phys Rev.* (2017) **C96**:014004. doi: 10.1103/PhysRevC.96.014004
47. Ruiz Arriola E, Ruiz de Elvira J. Coarse graining hadronic scattering. In: *9th International Workshop on Chiral Dynamics (CD18)*. Durham, NC (2019).
48. Navarro Perez R, Amaro JE, Ruiz Arriola E. Partial wave analysis of chiral NN interactions. *Few Body Syst.* (2014) **55**:983–7. doi: 10.1007/s00601-014-0817-3
49. Aviles JB. Delta-function model for the two-nucleon interaction. *Phys Rev.* (1972) **C6**:1467–84. doi: 10.1103/PhysRevC.6.1467
50. Entem DR, Ruiz Arriola E, Pavon Valderrama M, Machleidt R. Renormalization of chiral two-pion exchange NN interactions. momentum versus coordinate space. *Phys Rev.* (2008) **C77**:044006. doi: 10.1103/PhysRevC.77.044006
51. Navarro Perez R, Amaro JE, Ruiz Arriola E. Coarse graining nuclear interactions. *Prog Part Nucl Phys.* (2012) **67**:359–64. doi: 10.1016/j.ppnp.2011.12.044
52. Calogero F. *Variable Phase Approach to Potential Scattering by F Calogero*, Vol. 35. New York, NY: Elsevier (1967).
53. Navarro Perez R, Amaro JE, Ruiz Arriola E. Statistical error analysis for phenomenological nucleon-nucleon potentials. *Phys Rev.* (2014) **C89**:064006. doi: 10.1103/PhysRevC.89.064006
54. Navarro Pérez R, Amaro JE, Ruiz Arriola E. Error analysis of nuclear forces and effective interactions. *J Phys.* (2015) **G42**:034013. doi: 10.1088/0954-3899/42/3/034013
55. Puzikov L, Ryndin R, Smorodinsky J. Construction of the scattering matrix of a two-nucleon system. *Nucl Phys.* (1957) **3**:436–45.
56. Hoshizaki N. Formalism of nucleon-nucleon scattering. *Prog Theor Phys Suppl.* (1969) **42**:107–59. doi: 10.1143/PTPS.42.107
57. Bystricky J, Lehar F, Winternitz P. Formalism of nucleon-nucleon elastic scattering experiments. *J Phys.* (1978) **39**:1. doi: 10.1051/jphys:019780039010100
58. Binstock J, Bryan R. Test of peripherality for n-n scattering. *Phys Rev.* (1971) **D4**:1341–52. doi: 10.1103/PhysRevD.4.1341
59. Goldberger ML, Watson KM. *Collision Theory*. New York, NY: Courier Corporation (2004).
60. Navarro Pérez R, Amaro JE, Ruiz Arriola E. Precise determination of charge dependent pion-nucleon-nucleon coupling constants. *Phys Rev.* (2017) **C95**:064001. doi: 10.1103/PhysRevC.95.064001
61. Ruiz Arriola E, Amaro JE, Navarro Pérez R. Three pion nucleon coupling constants. *Mod Phys Lett.* (2016) **A31**:1630027. doi: 10.1142/S0217732316300275
62. Evans MJ, Rosenthal JS. *Probability and Statistics: The Science of Uncertainty*. New York, NY: Macmillan (2004).
63. Eadie WT, Drijard D, James FE. *Statistical Methods in Experimental Physics*. Amsterdam: North-Holland1 (1971).
64. Navarro Pérez R, Ruiz Arriola E, Ruiz de Elvira J. Self-consistent statistical error analysis of $\pi\pi$ scattering. *Phys Rev.* (2015) **D91**:074014. doi: 10.1103/PhysRevD.91.074014
65. Stoks V, de Swart JJ. Comparison of potential models with the pp scattering data below 350 MeV. *Phys Rev.* (1993) **C47**:761–7. doi: 10.1103/PhysRevC.47.761
66. Stoks VGJ, de Swart JJ. Comparison of potential models with the n p scattering data below 350-MeV. *Phys Rev.* (1995) **C52**:1698–701. doi: 10.1103/PhysRevC.52.1698
67. Calle Cordon A, Pavon Valderrama M, Ruiz Arriola E. Nucleon-nucleon interaction, charge symmetry breaking and renormalization. *Phys Rev.* (2012) **C85**:024002. doi: 10.1103/PhysRevC.85.024002
68. Nieves J, Ruiz Arriola E. Error estimates for pi pi scattering threshold parameters in chiral perturbation theory to two loops. *Eur Phys J.* (2000) **A8**:377–84. doi: 10.1007/s10050-000-4511-0
69. de Swart J, Rentmeester M, Timmermans R. The Status of the pion - nucleon coupling constant. *PiN Newslett.* (1997) **13**:96–107.
70. Sainio M. Pion nucleon coupling constant: working group summary. *PiN Newslett.* (1999) **15**:156–61.
71. Matsinos E. A brief history of the pion-nucleon coupling constant. *arXiv [Preprint]* arXiv:1901.01204 (2019).
72. Baru V, Hanhart C, Hoferichter M, Kubis B, Nogga A, Phillips DR. Precision calculation of the π^- deuteron scattering length and its impact on threshold π N scattering. *Phys Lett.* (2011) **B694**:473–7. doi: 10.1016/j.physletb.2010.10.028
73. Baru V, Hanhart C, Hoferichter M, Kubis B, Nogga A, Phillips DR. Precision calculation of threshold pi d scattering, pi N scattering lengths, and the GMO sum rule. *Nucl Phys.* (2011) **A872**:69–116. doi: 10.1016/j.nuclphysa.2011.09.015
74. Hoferichter M, Ruiz de Elvira J, Kubis B, Meißner UG. Roy–Steiner-equation analysis of pion–nucleon scattering. *Phys Rept.* (2016) **625**:1–88. doi: 10.1016/j.physrep.2016.02.002
75. Navarro Pérez R, Amaro JE, Ruiz Arriola E. The low-energy structure of the nucleon–nucleon interaction: statistical versus systematic uncertainties. *J Phys.* (2016) **G43**:114001. doi: 10.1088/0954-3899/43/11/114001
76. Birge RT. The calculation of errors by the method of least squares. *Phys Rev.* (1932) **40**:207.
77. Navarro Pérez R, Amaro JE, Ruiz Arriola E. Coarse grained NN potential with Chiral Two Pion Exchange. *Phys Rev.* (2014) **C89**:024004. doi: 10.1103/PhysRevC.89.024004

78. Machleidt R, Sammarruca F, Song Y. The non-local nature of the nuclear force and its impact on nuclear structure. *Phys Rev.* (1996) **C53**:1483–7. doi: 10.1103/PhysRevC.53.1483
79. Friar JL, Payne GL, Stoks VGJ, de Swart JJ. Triton calculations with the new Nijmegen potentials. *Phys Lett.* (1993) **B311**:4. doi: 10.1016/0370-2693(93)90523-K
80. Bethe HA. Theory of the effective range in nuclear scattering. *Phys Rev.* (1949) **76**:38–50. doi: 10.1103/PhysRev.76.38
81. Madsen LB. Effective range theory. *Am J Phys.* (2002) **70**:811–4. doi: 10.1119/1.1473644
82. Pavon Valderrama M, Ruiz Arriola E. Low-energy NN scattering at next-to-next-to-next-to-next-to-leading order for partial waves with $j \leq 5$. *Phys Rev.* (2005) **C72**:044007. doi: 10.1103/PhysRevC.72.044007
83. Navarro Pérez R, Amaro JE, Ruiz Arriola E. Bootstrapping the statistical uncertainties of NN scattering data. *Phys Lett.* (2014) **B738**:155–9. doi: 10.1016/j.physletb.2014.09.035
84. Epelbaum E, Glockle W, Meissner UG. The Two-nucleon system at next-to-next-to-next-to-leading order. *Nucl Phys.* (2005) **A747**:362–424. doi: 10.1016/j.nuclphysa.2004.09.107
85. Epelbaum E, Krebs H, Meißner UG. Improved chiral nucleon-nucleon potential up to next-to-next-to-next-to-leading order. *Eur Phys J.* (2015) **A51**:53. doi: 10.1140/epja/i2015-15053-8
86. Furnstahl RJ, Klco N, Phillips DR, Wesolowski S. Quantifying truncation errors in effective field theory. *Phys Rev.* (2015) **C92**:024005. doi: 10.1103/PhysRevC.92.024005
87. Navarro Perez R, Amaro JE, Ruiz Arriola E. Uncertainty quantification of effective nuclear interactions. *Int J Mod Phys.* (2016) **E25**:1641009. doi: 10.1142/S0218301316410093
88. Navarro Perez R, Amaro JE, Ruiz Arriola E. Effective interactions in the delta-shells potential. *Few Body Syst.* (2013) **54**:1487–90. doi: 10.1007/s00601-012-0537-5
89. Ruiz Arriola E. Low scale aturation of effective NN interactions and their symmetries. *Symmetry* (2016) **8**:42. doi: 10.3390/sym8060042
90. Bogner S, Kuo T, Schwenk A. Model independent low momentum nucleon interaction from phase shift equivalence. *Phys Rept.* (2003) **386**:1–27. doi: 10.1016/j.physrep.2003.07.001
91. Bogner S, Furnstahl R, Schwenk A. From low-momentum interactions to nuclear structure. *Prog Part Nucl Phys.* (2010) **65**:94–147. doi: 10.1016/j.ppnp.2010.03.001
92. Oka M, Yazaki K. Baryon baryon interaction from quark model viewpoint. *Int Rev Nucl Phys.* (1984) **1**:489–567. doi: 10.1142/9789814415132_0006
93. Alvarez-Estrada RF, Fernandez F, Sanchez-Gomez JL, Vento V. Models of hadron structure based on quantum chromodynamics. *Lect Notes Phys.* (1986) **259**:1–294.
94. Valcarce A, Garcilazo H, Fernandez F, Gonzalez P. Quark-model study of few-baryon systems. *Rept Prog Phys.* (2005) **68**:965–1042. doi: 10.1088/0034-4885/68/5/R01
95. Weinberg S. Nuclear forces from chiral Lagrangians. *Phys Lett.* (1990) **B251**:288–92. doi: 10.1016/0370-2693(90)90938-3
96. Bedaque PF, van Kolck U. Effective field theory for few nucleon systems. *Ann Rev Nucl Part Sci.* (2002) **52**:339–96. doi: 10.1146/annurev.nucl.52.050102.090637
97. Epelbaum E, Hammer HW, Meissner UG. Modern theory of nuclear forces. *Rev Mod Phys.* (2009) **81**:1773–825. doi: 10.1103/RevModPhys.81.1773
98. Machleidt R, Entem DR. Chiral effective field theory and nuclear forces. *Phys Rept.* (2011) **503**:1–75. doi: 10.1016/j.physrep.2011.02.001
99. Kaiser N, Brockmann R, Weise W. Peripheral nucleon-nucleon phase shifts and chiral symmetry. *Nucl Phys.* (1997) **A625**:758–88. doi: 10.1016/S0375-9474(97)00586-1
100. Rentmeester MCM, Timmermans RGE, Friar JL, de Swart JJ. Chiral two pion exchange and proton proton partial wave analysis. *Phys Rev Lett.* (1999) **82**:4992–5. doi: 10.1103/PhysRevLett.82.4992
101. Rentmeester MCM, Timmermans RGE, de Swart JJ. Determination of the chiral coupling constants c(3) and c(4) in new pp and np partial wave analyses. *Phys Rev.* (2003) **C67**:044001. doi: 10.1103/PhysRevC.67.044001
102. Entem DR, Machleidt R. Chiral 2pi exchange at order four and peripheral NN scattering. *Phys Rev.* (2002) **C66**:014002. doi: 10.1103/PhysRevC.66.014002
103. Entem DR, Machleidt R. Accurate charge dependent nucleon nucleon potential at fourth order of chiral perturbation theory. *Phys. Rev.* (2003) **C68**:041001. doi: 10.1103/PhysRevC.68.041001
104. Navarro Pérez R, Amaro JE, Ruiz Arriola E. Low energy chiral two pion exchange potential with statistical uncertainties. *Phys Rev.* (2015) **C91**:054002. doi: 10.1103/PhysRevC.91.054002
105. Carlsson BD, Ekström A, Forssén C, Strömberg DF, Jansen GR, Lilja O, et al. Uncertainty analysis and order-by-order optimization of chiral nuclear interactions. *Phys Rev.* (2016) **X6**:011019. doi: 10.1103/PhysRevX.6.011019
106. Piarulli M, Girlanda L, Schiavilla R, Kievsky A, Lovato A, Marcucci LE, et al. Local chiral potentials with Δ-intermediate states and the structure of light nuclei. *Phys Rev.* (2016) **C94**:054007. doi: 10.1103/PhysRevC.94.054007
107. Reinert P, Krebs H, Epelbaum E. Semilocal momentum-space regularized chiral two-nucleon potentials up to fifth order. *Eur Phys J.* (2018) **A54**:86. doi: 10.1140/epja/i2018-12516-4
108. Entem DR, Machleidt R, Nosyk Y. High-quality two-nucleon potentials up to fifth order of the chiral expansion. *Phys Rev.* (2017) **C96**:024004. doi: 10.1103/PhysRevC.96.024004
109. Ruiz Arriola E, Amaro JE, Navarro Perez R. The falsification of chiral nuclear forces. *EPJ Web Conf.* (2017) **137**:09006. doi: 10.1051/epjconf/201713709006
110. Simo IR, Amaro JE, Ruiz Arriola E, Navarro Pérez R. Low energy peripheral scaling in nucleon–nucleon scattering and uncertainty quantification. *J Phys.* (2018) **G45**:035107. doi: 10.1088/1361-6471/aaabd2
111. Entem DR, Kaiser N, Machleidt R, Nosyk Y. Peripheral nucleon-nucleon scattering at fifth order of chiral perturbation theory. *Phys Rev.* (2015) **C91**:014002. doi: 10.1103/PhysRevC.91.014002
112. Shirokov AM, Vary JP, Mazur AI, Weber TA. Realistic Nuclear Hamiltonian: 'Ab exitu' approach. *Phys Lett.* (2007) **B644**:33–7. doi: 10.1016/j.physletb.2006.10.066
113. Johnson CW. Many-body fits of phase-equivalent effective interactions. *Phys Rev.* (2010) **C82**:031303. doi: 10.1103/PhysRevC.82.031303
114. Blatt JM, Weisskopf VF. *Theoretical Nuclear Physics.* New York, NY: Springer (1952). doi: 10.1007/978-1-4612-9959-2
115. Leun CVD, Alderliesten C. The deuteron binding energy. *Nucl Phys.* (1982) **A380**:261–9. doi: 10.1016/0375-9474(82)90105-1
116. Borbély I, Grüebler W, König V, Schmelzbach PA, Mukhamedzhanov AM. Determination of the deuteron s-state asymptotic normalization by continuation of p-d elastic cross section to the transfer pole. *Phys Lett.* (1985) **160B**:17–20. doi: 10.1016/0370-2693(85)91459-5
117. Rodning NL, Knutson LD. Asymptotic D-state to S-state ratio of the deuteron. *Phys Rev.* (1990) **C41**:898–909. doi: 10.1103/PhysRevC.41.898
118. Klarsfeld S, Martorell J, Oteo JA, Nishimura M, Sprung DWL. Determination of the deuteron mean square radius. *Nucl Phys.* (1986) **A456**:373–96. doi: 10.1016/0375-9474(86)90400-8
119. Bishop DM, Cheung LM. Quadrupole moment of the deuteron from a precise calculation of the electric field gradient in D-2. *Phys Rev.* (1979) **A20**:381–4. doi: 10.1103/PhysRevA.20.381
120. de Swart JJ, Terheggen CPF, Stoks VGJ. The Low-energy n p scattering parameters and the deuteron. In: *3rd International Symposium on Dubna Deuteron 95.* Dubna (1995).
121. Gilman R, Gross F. Electromagnetic structure of the deuteron. *J Phys G* (2002) **28**:R37. doi: 10.1088/0954-3899/28/4/201
122. Navarro Perez R, Amaro JE, Ruiz Arriola E. Nucleon-nucleon chiral two pion exchange potential vs coarse grained interactions. In: *Presented by R. Navarro Perez at the The 7th International Workshop on Chiral Dynamics.* Newport News, VA (2013). p. 104. doi: 10.22323/1.172.0104
123. Nogga A, Kamada H, Gloeckle W. Modern nuclear force predictions for the alpha particle. *Phys Rev Lett.* (2000) **85**:944–7. doi: 10.1103/PhysRevLett.85.944
124. Perne R, Kroger H. Tjon line in few-body systems. *Phys Rev.* (1979) **C20**:340–4. doi: 10.1103/PhysRevC.20.340

125. Tjon JA. The three and four nucleon systems (theory). *Nucl Phys.* (1981) **A353**:47–60. doi: 10.1016/0375-9474(81)90698-9
126. Nogga A, Bogner SK, Schwenk A. Low-momentum interaction in few-nucleon systems. *Phys Rev.* (2004) **C70**:061002. doi: 10.1103/PhysRevC.70.061002
127. Klein N, Elhatisari S, Lähde TA, Lee D, Meißner UG. The Tjon band in nuclear lattice effective field theory. *Eur Phys J.* (2018) **A54**:121. doi: 10.1140/epja/i2018-12553-y
128. Delfino A, Frederico T, Timoteo VS, Tomio L. The Few scales of nuclei and nuclear matter. *Phys Lett.* (2006) **B634**:185. doi: 10.1016/j.physletb.2006.01.046
129. Ruiz Arriola E, Szpigel S, Timoteo VS. Fixed points of the similarity renormalization group and the nuclear many-body problem. *Few Body Syst.* (2014) **55**:971–5. doi: 10.1007/s00601-014-0858-7
130. Ruiz Arriola E, Szpigel S, Timóteo VS. Fixed points of the SRG evolution and the on-shell limit of the nuclear force. *Ann Phys.* (2016) **371**:398–436. doi: 10.1016/j.aop.2016.06.002
131. Shirokov AM, Kulikov VA, Mazur AI, Vary JP, Maris P. Deuteron-equivalent and phase-equivalent interactions within light nuclei. *Phys Rev.* (2012) **C85**:034004. doi: 10.1103/PhysRevC.85.034004
132. Rozpedzik D, Golak J, Skibinski R, Witala H, Glockle W, Epelbaum E, et al. A first estimation of chiral four-nucleon force effects in He-4. *Acta Phys Pol.* (2006) **B37**:2889–904. Available online at: https://www.actaphys.uj.edu.pl/R/37/10/2889/pdf
133. Epelbaum E. Four-nucleon force using the method of unitary transformation. *Eur Phys J.* (2007) **A34**:197–214. doi: 10.1140/epja/i2007-10496-0
134. Moshinsky M. Short range forces and nuclear shell theory. *Nucl Phys.* (1958) **8**:19–40.
135. Skyrme T. The effective nuclear potential. *Nucl Phys.* (1958) **9**:615–34.
136. Vautherin D, Brink DM. Hartree-Fock calculations with Skyrme's interaction. 1. Spherical nuclei. *Phys Rev.* (1972) **C5**:626–47. doi: 10.1103/PhysRevC.5.626
137. Negele JW, Vautherin D. Density-matrix expansion for an effective nuclear hamiltonian. *Phys Rev.* (1972) **C5**:1472–93. doi: 10.1103/PhysRevC.5.1472
138. Chabanat E, Meyer J, Bonche P, Schaeffer R, Haensel P. A Skyrme parametrization from subnuclear to neutron star densities. *Nucl Phys.* (1997) **A627**:710–46. doi: 10.1016/S0375-9474(97)00596-4
139. Bender M, Heenen PH, Reinhard PG. Self-consistent mean-field models for nuclear structure. *Rev Mod Phys.* (2003) **75**:121–80. doi: 10.1103/RevModPhys.75.121
140. Friedrich J, Reinhard PG. Skyrme-force parametrization: least-squares fit to nuclear ground-state properties. *Phys Rev.* (1986) **C33**:335–51. doi: 10.1103/PhysRevC.33.335
141. Klupfel P, Reinhard PG, Burvenich TJ, Maruhn JA. Variations on a theme by Skyrme: a systematic study of adjustments of model parameters. *Phys Rev.* (2009) **C79**:034310. doi: 10.1103/PhysRevC.79.034310
142. Ruiz Arriola E. Low scale saturation of effective NN interactions and their symmetries (2010).
143. Bethe HA. Nuclear many-body problem. *Phys Rev.* (1956) **103**:1353–90. doi: 10.1103/PhysRev.103.1353
144. Goldstone J. Derivation of the brueckner many-body theory. *Proc R Soc Lond.* (1957) **A239**:267–79. doi: 10.1098/rspa.1957.0037
145. Ruiz Simo I, Navarro Perez R, Amaro JE, Ruiz Arriola E. Coarse grained short-range correlations. *Phys Rev.* (2017) **C95**:054003. doi: 10.1103/PhysRevC.95.054003
146. Ruiz Simo I, Navarro Pérez R, Amaro JE, Ruiz Arriola E. Coarse graining the Bethe–Goldstone equation: nucleon–nucleon high-momentum components. *Phys Rev.* (2017) **C96**:054006. doi: 10.1103/PhysRevC.96.054006
147. Amaro JE, Navarro Perez R, Ruiz Arriola E. Error analysis of nuclear matrix elements. *Few Body Syst.* (2014) **55**:977–81. doi: 10.1007/s00601-013-0756-4
148. Neff T, Feldmeier H. Tensor correlations in the unitary correlation operator method. *Nucl Phys.* (2003) **A713**:311–71. doi: 10.1016/S0375-9474(02)01307-6

Conflict of Interest: The authors declare that the research was conducted in the absence of any commercial or financial relationships that could be construed as a potential conflict of interest.